THE UNIVERSITY OF QUEENSLAND

AUSTRALIA

Subclinical left ventricular myocardial dysfunction in non-obstructive coronary artery disease

Shi Yi Goo

BPharm, MBBS (Hons)

A thesis submitted for the degree of Master of Philosophy at

The University of Queensland in 2019

Faculty of Medicine

ABSTRACT

Background

There is increasing evidence that accumulation of ectopic fat in the heart such as epicardial adipose tissue (EAT) contribute to cardiovascular disease and myocardial dysfunction. These ectopic fat play important physiological roles in the regulation of glucose metabolism and as an energy source. However, in pathological conditions, they are pro-inflammatory and secrete adipokines, which could accelerate atherosclerosis and cardiac remodeling. As these ectopic fats are well linked to conventional cardiovascular risk factors, previous studies have mainly investigated its association with coronary artery disease (CAD). The effects of EAT and non-obstructive coronary atherosclerosis on left ventricular (LV) myocardial function in those with preserved ejection fraction (EF) independent of other confounders such as diabetes and hypertension are unknown.

Aims

The main aim of this research is to investigate the effect of EAT and non-obstructive coronary atherosclerosis on subclinical LV myocardial function using two-dimensional (2D) and three-dimensional (3D) speckle tracking echocardiography (STE) in patients with preserved LV EF.

Methods

In the first study, 130 patients (53 ± 9 years, 53.1% male) with non-obstructive CAD (defined as <50% coronary stenosis by cardiac contrasted-enhanced CT) and preserved LV EF were enrolled prospectively. EAT volume was measured by cardiac CT and multidirectional global strains were evaluated by 3D STE.

In the second study, 96 patients (51 ± 8.6 years, 56% male) without significant CAD, hypertension and diabetes were enrolled prospectively. The exclusion of patients with hypertension and diabetes eliminate other known confounders of LV strains. LV strains were evaluated by 2D and 3D STE.

Multivariable analyses were performed to investigate independent determinants of 2D and 3D multidirectional strains in each study. Additional analyses were performed to compare the predictive value of 2D versus 3D GLS for the presence of coronary atherosclerosis.

Results

In the first study, EAT volume measured by cardiac computed tomography (CT) was independently associated with 3D global longitudinal strain (GLS, $r = 0.601$; $p < 0.001$), global circumferential strain (GCS, $r = 0.375$; $p < 0.001$), global radial strain (GRS, $r = -0.546$; $p < 0.001$), and global area strain (GAS, $r = 0.558$; $p < 0.001$). In multivariable analyses, EAT volume was the strongest predictor of 3D GLS (standardized $\beta = 0.512$; $p < 0.001$), GCS (standardized $\beta = 0.242$; $p = 0.006$), GRS (standardized $\beta = -0.422$; $p < 0.001$), and GAS (standardized $\beta = 0.428$; $p < 0.001$). In contrast, other measures of obesity including BMI and waist/hip ratio were not independent determinants of 3D multidirectional global strain (all $p > 0.05$).

In the second study, patients with non-obstructive CAD had lower 2D GLS (-18.5 ± 2.2% vs. -20.1 ± 1.9%, $p < 0.001$) and 3D GLS (-14.9 ± 2.4% vs. -16.3 ± 3.1%, $p = 0.011$) compared to those without any coronary atherosclerosis. In multivariable analyses model using 2D GLS, both age (odd ratio = 2.16, $p = 0.011$) and 2D GLS (odd ratio = 1.55, $p = 0.001$) were independent determinants of non-obstructive coronary atherosclerosis. When 2D GLS was replaced with 3D GLS in similar analyses, both age (odd ratio = 2.23, $p = 0.007$) and 3D GLS (odd ratio =1.21, $p = 0.027$) were also independent determinants of coronary

atherosclerosis. These associations were independent of obstructive CAD, diabetes and hypertension. 2D GLS was superior to 3D GLS in detecting coronary atherosclerosis using decision curve analysis despite having similar receiver operating characteristic curve derived area under the curves (2D GLS: 0.70 vs. 3D GLS: 0.65, $p > 0.05$).

Conclusions

EAT and non-obstructive coronary atherosclerosis are independent determinants of subclinical myocardial dysfunction, independent of significant CAD, diabetes and hypertension. Future studies are needed to explore the potential role of reducing EAT volume and management of early coronary atherosclerosis in prevention of progression of myocardial dysfunction especially in patients with metabolic and diabetic heart disease.

DECLARATION OF AUTHORS

This thesis is composed of my original work, and contains no material previously published or written by another person except where due reference has been made in the text. I have clearly stated the contribution by others to jointly-authored works that I have included in my thesis.

I have clearly stated the contribution of others to my thesis as a whole, including statistical assistance, survey design, data analysis, significant technical procedures, professional editorial advice, and any other original research work used or reported in my thesis. The content of my thesis is the result of work I have carried out since the commencement of my research higher degree candidature and does not include a substantial part of work that has been submitted to qualify for the award of any other degree or diploma in any university or other tertiary institution. I have clearly stated which parts of my thesis, if any, have been submitted to qualify for another award.

I acknowledge that an electronic copy of my thesis must be lodged with the University Library and, subject to the policy and procedures of The University of Queensland, the thesis be made available for research and study in accordance with the Copyright Act 1968 unless a period of embargo has been approved by the Dean of the Graduate School.

I acknowledge that copyright of all material contained in my thesis resides with the copyright holder(s) of that material. Where appropriate I have obtained copyright permission from the copyright holder to reproduce material in this thesis.

PUBLICATIONS INCLUDED IN THIS THESIS

1. Ng AC, Goo SY, Roche N, van der Geest RJ, Wang WY. Epicardial Adipose Tissue Volume and Left Ventricular Myocardial Function Using 3-Dimensional Speckle Tracking Echocardiography. Can J Cardiol. 2016;32(12):1485-92.

Contributor	**Statement of contribution**
Shi Yi Goo	Conception and design of the project (50%) Collection and analysis of research data Co-wrote and joint first author of study 1

SUBMITTED MANUSCRIPTS INCLUDED IN THIS THESIS

No manuscripts submitted for publication.

OTHER PUBLICATIONS DURING CANDIDATURE

1. Ng AC, Goo SY, Roche N, van der Geest RJ, Wang WY. Epicardial Adipose Tissue Volume and Left Ventricular Myocardial Function Using 3-Dimensional Speckle Tracking Echocardiography. Can J Cardiol. 2016;32(12):1485-92.

CONTRIBUTION OF OTHERS TO THE THESIS

Contributor	Statement of contribution
Associate Professor Arnold Ng	Conception and design of the project (50%) Co-wrote and joint first author of study 1 Critical revision of study 2
Associate Professor William Wang	Critical revision of study 2

STATEMENT OF PARTS OF THE THESIS SUBMITTED TO QUALIFY FOR THE AWARD OF ANOTHER DEGREE

No works submitted towards another degree have been included in this thesis**.**

RESEARCH INVOLVING HUMAN OR ANIMAL SUBJECTS

The Princess Alexandra Hospital Metro South Hospital and Health Service Human Research Ethics Committee has approved this study (HREC/12/QPAH/563).

ACKNOWLEGEMENTS

I hereby acknowledge the academic input and support of my advisors, Associate Professor Arnold Ng and Associate Professor William Wang.

FINANCIAL SUPPORT

No financial support was provided to fund this research.

KEYWORDS

coronary artery disease, left ventricular function, strain.

AUSTRALIAN AND NEW ZEALAND STANDARD RESEARCH CLASSIFICATION (ANZSRC)

ANZSRC code: 110201, Cardiology, 100%

FIELDS OF RESEARCH (FoR) CLASSIFICATION

FoR code: 1102, Cardiovascular medicine and haematology, 100%

TABLE OF CONTENT

LIST OF ABRREVIATIONS

BMI	Body mass index
BP	Blood pressure
CAD	Coronary artery disease
CMR	Cardiac magnetic resonance imaging
CS	Circumferential strain
CT	Computed tomography
EAT	Epicardial adipose tissue
ECG	Electrocardiogram
EDVI	End-diastolic volume index
ESVI	End-systolic volume index
eGFR	Glomerular filtration rate
EF	Ejection fraction
GAS	Global area strain

GCS	Global circumferential strain
GLS	Global longitudinal strain
GRS	Global radial strain
HBA1c	Glycated haemoglobin
HDL	High density lipoprotein
LDL	Low density lipoprotein
LS	Longitudinal strain
LV	Left ventricle/ventricular
RS	Radial strain
STE	Speckle-tracking echocardiography
TG	Triglyceride
2D	2-dimensional
3D	3-dimensional

CHAPTER ONE

Introduction

Diabetes, hypertension, hypercholesterolaemia, obesity and obstructive coronary artery disease (CAD) are well-recognized risk factors for myocardial dysfunction (1-3). There is increasing evidence that ectopic accumulation of fat in the heart can increase cardiovascular risk and cause left ventricular (LV) dysfunction (4, 5).

This review will focus on the effect of cardiac ectopic fat such as epicardial adipose tissue (EAT) and non-obstructive coronary atherosclerosis on LV myocardial function. The role of two-dimensional (2D) and three-dimensional (3D) speckle-tracking echocardiography (STE) in the detection of subclinical myocardial dysfunction will also be discussed.

1.1 Literature review

1.1.1 Ectopic Fat

Ectopic fat is defined by excess adipose tissue in locations not classically associated with adipose tissue storage (6-8). In the heart, ectopic fat can accumulate in three different locations: intramyocardial, epicardial (bounded between the epicardium and the visceral pericardium) and pericardial (defined as external to the parietal pericardium) (6-8).

1.1.2 Epicardial adipose tissue

EAT is the true visceral fat depot of the heart that is derived from the splanchnopleuric mesoderm associated with the gut (2, 9). It is of the same embryologic origin as mesenteric and omental fat cells, having evolved from brown adipose tissue during embryogenesis (2, 9). In human heart, EAT is commonly found in the atrioventricular and interventricular grooves (10-12). As no muscle fascia divides the epicardial fat and

myocardium, they share the same circulation (10, 12, 13). Its close anatomical proximity to the myocardium and coronary arteries leads to it having a dynamic effect on the working of the heart (12, 14-16).

Under normal conditions, EAT is thought to serve a number of physiologic functions, including acting as an energy source to the myocardium (17, 18). Epicardial adipocytes are smaller in size than other fat depots (19). They possess different fatty acids composition and have higher rates of free fatty acids synthesis, uptake and release but lower rates of glucose utilization (19). This serves to capture and store intravascular free fatty acids to protect cardiac myocytes from exposure to excessive coronary arterial free fatty acids concentrations during increased energy intake and, at other times to release these fatty acids during periods of need (12, 20-23). However, it is only when the adipose tissues become dysfunctional, the term "lipotoxicity" is used to describe this impairment in tissue homeostasis attributable to alterations in lipid utilization, or lipid-induced changes in intracellular signaling (24). It has been proposed that cardiac lipotoxicity promote vascular endothelial and cardiac dysfunction through multiple synergistic signaling pathways such as microRNAs, epigenetic regulations and mitochondrial function (24).

In addition, EAT has been shown to produce several anti-inflammatory and anti-atherogenic adipokines, such as adiponectin and adrenomedullin (10, 12, 16, 25, 26). However, it is a visceral fat deposit and as such has the capacity to secrete a number of cytokines and chemokines with pro-inflammatory and pro-atherogenic properties such as tumour necrosis factor-alpha, interleukin-6, resistin, leptin, plaminogen activator inhibitor-1 and angiotensinogen (16, 23, 25, 27-29). What influences this equilibrium between harmful and possible protective effects is still unknown and is the key to understanding the pathophysiology of EAT and its link to cardiac lipotoxicity (11).

1.1.2.1 Epicardial adipose tissue and coronary atherosclerosis

1.1.2.1.1 Pathophysiology

Most of the studies on the pathophysiology of EAT on cardiovascular disease stemmed from its association with atherosclerosis and vascular inflammation through its paracrine, vasocrine and mechanical effects (15, 16, 28, 30-33).

EAT is ideally situated to have a paracrine effect on coronary arterioles as these is no tissue separating EAT and these blood vessels (16). In vivo studies where inflammatory cytokines were experimentally applied to the arterial adventitia have been shown to cause inflammatory changes by diffusion into the intimal layer (34, 35). Subsequently, both animal (21) and human studies confirmed the paracrine effect of EAT in promoting vascular inflammation (10, 36, 37). In particular, Mazurek and coworkers demonstrated inflammation was increased in EAT when compared to peripheral subcutaneous fat in patients with critical CAD undergoing coronary bypass graft surgery (36). Other studies also found an increase of CD45 mRNA expression in the EAT of subjects with CAD, representing elevated macrophage infiltration and a shift towards pro-inflammatory subpopulation of macrophages (38, 39) as well as an increase of mast cells and leucocyte common antigen positive cells in the adventitia of coronary lesions (40-42).

Further evidence supporting the paracrine effect of EAT on development of CAD came from the studies of intramyocardial segments of coronary arteries (43-45). These intramyocardial segments are usually not surrounded by EAT and tend to be free of atherosclerotic lesions while the “kinked” segments surrounded by EAT often have atherosclerotic plaques (43-45).

Additionally, adipokines and free fatty acids might be released from EAT directly into the vasa vasorum and be transported downstream into the arterial wall according to a “vasocrine signalling” mechanism (15). EAT may also take part in regulation of

vasoconstriction and vascular smooth muscle cell proliferation in coronary arteries. This hypothesis was derived from experimental studies that showed the release of relaxing factor(s) and protein growth factor(s) from perivascular fat (43-46). These factors exert anti-contractile effect on smooth muscle cell and promote proliferation of smooth muscle cells (43-46).

EAT might also contribute to atherosclerosis through specific mechanical effects (47). For instance, under physiological conditions, EAT could attenuate coronary artery torsion (48). However, the presence of atherosclerotic plaque in coronary arteries leads to an asymmetric expansion of the vessel wall, known as positive vessel remodeling (48). Because of its intrinsic compressibility, EAT has therefore been suggested to play a permissive role in vessel expansion where coronary lesions surrounded by EAT can expand more easily (48).

1.1.2.1.2 Clinical studies

There is a correlation between EAT and coronary atherosclerosis in patients with established CAD (49-52), suspected CAD (53-57), symptomatic patients with low-intermediate risk of CAD (57-63), asymptomatic patients with low-intermediate risk of CAD (64, 65), and even in healthy patients (66-69). Interestingly, both Alexopoulos and coworkers and Oka and coworkers found that larger EAT volume was associated with non-calcified plaques compared to calcified plaques (57, 58). These non-calcified plaques were thought to be a feature of coronary vulnerability (57, 58).

A few studies have explored the relationship between EAT and coronary flow, which could indicate microvascular dysfunction and hence early atherosclerosis (13, 70-72). It was found that EAT correlated with reduced coronary flow reserve in patients with angina or electrocardiographic evidence of CAD but whose coronary arteries were angiographically normal (13, 70, 71). This could be secondary to vasoconstriction induced by EAT (43-46).

In contrast, some studies did not demonstrate a correlation between EAT and CAD (73-75). Chaowalit and coworkers found no association between EAT thickness measured by 2D echocardiography and CAD on angiography (73). The authors suggested that the biochemical, cellular and other functional characteristics of EAT might be more important in the pathophysiology of CAD than the total amount of EAT (73). Secondly, because EAT has a heterogeneous distribution around the heart, the 2D linear quantification of EAT may not be an accurate measurement for the total amount of EAT (11, 73).

1.1.2.2 Epicardial adipose tissue and left ventricular function

1.1.2.2.1 Pathophysiology

Increased visceral adiposity is one of the causes of adverse LV remodeling (76-79). Therefore, EAT may be a potential determinant of LV dysfunction. The effect of EAT on cardiac remodeling could be through its effect on coronary arteries as discussed in the previous section, or it could be a direct independent insult to the myocardium leading to enhanced myocardial hypertrophy, myocardial and perivascular fibrosis (6).

Autopsy and echocardiographic studies have shown that increasing EAT was associated with increasing LV mass that was independent of ischaemia (14, 80). The mechanism for such an association is unclear, but could be due to a combination of different factors (81). This includes the possible mechanical role of EAT in restricting the heart leading to decreased diastolic filling and atrial dilatation (82, 83). Additionally, the release of adipokines from EAT can induce cardiac remodeling and fibrosis (84, 85).

Another mechanism linking EAT and myocardial dysfunction may be secondary to the intracellular accumulation of triglycerides (TG) and toxic products of free fatty acids and intermediate lipid metabolism (86). Free fatty acids are the major source of energy for the myocardium (87). Under normal conditions, the majority of free fatty acids undergo rapid

oxidation and little is stored (87). Under conditions of excess fatty acids, however, they are stored as TG and result in cardiac steatosis (87). When the amount of free acid accumulation exceeds the cellular oxidative capacity, free fatty acids are shunted into non-oxidative pathways, leading to accumulation of toxic intermediates such as diacylglycerol and ceramide that disrupt cellular signaling, eventually leading to cellular apoptosis, fibrosis and myocardial contractile dysfunction (87). Both animal and human studies have provided consistent evidence that these intracellular changes were associated with increased LV mass, impaired LV function and cardiac fibrosis (88-93). It has been suggested that free fatty acids could directly diffuse from EAT into myocardial cells, exacerbating myocardial steatosis and lipotoxicity, leading to adverse structural and functional cardiac adaptations (15, 94, 95).

EAT also can affect the heart through its systemic effects. It is closely associated with insulin resistance and glucose intolerance, and these conditions could also predispose independently to derangements in LV mass and function (81).

1.1.2.2.2 Clinical studies

In small studies of healthy subjects with varying body mass indices, EAT thickness was found to be the strongest anthroprometric determinant of LV mass (7, 80). Similarly, larger population studies found that EAT volume was positively correlated with higher LV mass and larger left atrial dimension (82, 96). Subsequent studies in patients with conventional cardiovascular risk factors or CAD have also demonstrated an association between EAT, LV mass and diastolic dysfunction. For example, obese subjects with increased EAT had higher LV mass, impaired diastolic filling and enlarged atria, even after adjustment for body mass index (BMI), age and sex (84, 97, 98). Importantly, the amount and distribution of EAT vary widely between persons and are not strictly related to BMI or obesity (99).

In untreated hypertensive patients, EAT was an independent predictor of LV mass (100, 101) and diastolic dysfunction (6, 102). In a small study of 43 patients, EAT and presence of hypertension were independently correlated with Tei index, a Doppler-based measurement of LV systolic and diastolic functions (23). Similarly, EAT was also related to LV diastolic dysfunction in patients with no previous history of CAD (81, 103), suspected or known CAD (75, 104, 105), as well as patients with metabolic syndrome (83, 106).

Interestingly, a few recent studies have demonstrated that EAT was reduced in patients with established mild to severe systolic dysfunction [LV ejection fraction (EF) < 55%] (107-110). For example, Doesch and coworkers and Tabacki and coworkers enrolled patients with non-ischaemic dilated cardiomyopathy and found lower EAT burden in these patients (111, 112). The commonly observed lean and fat mass loss in patients with heart failure may explain the lower EAT volume in these patients (113). It has been postulated that as the myocardium becomes more dysfunctional and develops abnormal metabolic needs, the role of EAT as a source of energy or cytokine homeostasis would decrease, and as such, less would be found (36, 38, 109, 111). Additionally, natriuretic peptides seem to activate lipolysis in adipose tissue in patients with chronic heart failure (10). Consequently, increased level of such peptides contribute to decreased EAT volume in patients with chronic heart failure (112). These findings suggested a more complex interaction of regulatory pathways between EAT and myocardial contractile function.

A point to note is the main difference between studies showing reduced EAT in systolic dysfunction used EAT volume as the measurement parameter (108-112) whereas the studies with opposing results focused on linear EAT thickness measured using 4 chambers echocardiographic view (81, 112, 114). This was highlighted by Fluchter and coworkers who showed that “traditional” 2D echocardiographic EAT thickness measurements correlated poorly with 3D EAT volume measured by cardiac magnetic resonance imaging (CMR) in

patients with systolic dysfunction, suggesting EAT has an asymmetrical distribution in the heart (107).

1.1.2.3 Measurement of epicardial adipose tissue

Numerous studies have measured EAT using various modalities including echocardiography (11, 59), CT (33), and CMR (58) while focusing on different measurement techniques (thickness or volume) (33). To further clarify the relationship between EAT and the development of cardiovascular disease, it is important to accurately and reproducibly quantify this adipose tissue.

1.1.2.3.1 Echocardiography

Standard parasternal long-axis and short-axis views from 2D images permit measurement of EAT thickness overlying the right ventricular free wall (9, 11). EAT is generally identified as the relatively echo-free space between the outer wall of the myocardium and the visceral layer of pericardium; its thickness is measured perpendicularly on the free wall of the right ventricle at end-systole in 3 cardiac cycles (11). EAT thickness in the short axis view (instead of 4 chambers view) has been shown to correlate well with EAT mass (107).

Quantification of EAT by echocardiography has several advantages (11). Firstly, it is a direct measure of visceral fat deposition. Secondly, it is non-invasive, readily available, and less expensive than CT or CMR. Thirdly, it can be quantified in conjunction with other echocardiographic parameters such as LV mass and EF, which are traditionally associated with cardiovascular risks (11).

However, it is limited due to its dependence on the acoustic window and provides only 2D linear measurement (11, 64). Therefore, this measurement may not reflect the

variability of EAT thickness or total EAT volume (11). In addition, there is poor reproducibility (115). Other potential limitations of echocardiography also include difficulty in differentiating between epicardial and pericardial fat (11).

1.1.2.3.2 Cardiac computed tomography

EAT can be quantified by CT on the basis of thresholds for CT attenuation (99). The software produces an accurate volume of EAT by adding EAT areas of 25 to 30 sections and multiplying by slice thickness (33). Different anatomic boundaries for measurement of total EAT volumes have been reported and include the pulmonary artery bifurcation, the mid left atrium, and the aortic root as upper boundaries and the diaphragm and the left ventricular apex as lower boundaries (99).

The advantages of CT are its accuracy due to high spatial resolution and reproducibility (15, 33, 64, 116, 117). Furthermore, the pericardium is readily identified, resulting in easy differentiation between epi- and pericardial adipose tissue (66, 117). However, its drawbacks are it is time consuming and exposes patients to radiation (33, 59, 107).

1.1.2.3.3 Cardiac magnetic resonance imaging

The benefit of CMR is similar to CT when compared to echocardiographic measurement of EAT. Its superiority over CT is lack of harmful radiation exposure. Similar to CT measurement of EAT volume, regions of interest are manually drawn along the borders of fat surrounding the heart from the apex to the pulmonary trunk (118). EAT areas are multiplied by slice thickness and can be converted in grams by using fat density of 0.9196 g/ml as previously published (119). Its disadvantages include long scan time and known

contraindications to magnetic resonance imaging such as non-magnetic resonance compatible implantable devices, severe claustrophobia and severe renal impairment (120).

1.1.3 Assessment of left ventricular myocardial function

LV EF is the most commonly used clinical measurement of LV systolic function (121). However, it has several limitations. First, it does not always reflect intrinsic myocardial function (121). Secondly, it has limited prognostic value in the low-normal or higher range (122). Thirdly, any reduction in EF represents advanced LV functional impairment (123). Therefore, assessment of myocardial strain and strain rate using STE has gained recent popularity as it allows early detection of subclinical LV myocardial dysfunction (123). This opens the door to more aggressive treatment of early disease, rather than treatment of risk factors alone (124).

1.1.4 Speckle tracking echocardiography

Myocardial deformation analysis has evolved from one-dimensional assessment using tissue Doppler imaging to 2D and 3D STE (125, 126).

STE is based on an analysis of the spatial dislocation (referred to as tracking) of speckles (defined as spots generated by the interaction between the ultrasound beam and myocardial fibres) on routine echocardiographic images (127). This allows semi-automated quantification of myocardial deformation (i.e. strain and strain rate) in 3 spatial directions: longitudinal, circumferential and radial (123). In addition, STE also permits quantization of LV rotation and torsion (127). STE has been proven to provide incremental value beyond LV EF in predicting cardiac events and prognosis in various cardiac disorders (124).

1.1.4.1 Two-dimensional speckle-tracking echocardiography

2D STE measurements have been shown to correlate well with data obtained with tagged magnetic resonance imaging (the current "gold standard" for deformation analysis), both in normal myocardial segments and infarcted areas (128).

1.1.4.1.1 Limitations of two-dimensional speckle-tracking echocardiography

The whole heart moves through the 2D plane of interest due to torsion. Therefore, the 2D plane of interest disappears through the cardiac cycle, and is known as the "through-plane" or "out-of plane phenomenon" (121). This cause artefact in 2D STE.

In addition, technical factors such as image quality, choice of segmentation model, selection of image clip, fiducial landmarks and segmental contouring as well as region of interest can affect strain values (129). The variability of strain can also stem from intervendor and interobserver/intraobserver repeating testing (130). Previous studies on 2D STE have shown significant between and within manufacturer variability in measurements; this has impeded the transition of strain imaging from a research to a clinical tool in the past. However, Farsalinos and co-authors recently demonstrated the small differences between vendors and inter- and intraobserver were comparable to that of measurement of LV EF (131).

1.1.4.2 Three-dimensional speckle-tracking echocardiography

3D STE has recently been introduced as a method to measure cardiac deformation and volumes, and preliminary results have shown 3D STE indices detect subclinical LV dysfunction in those with risk factors for heart failure (132).

Compared to 2D STE, which cannot track myocardial motion occurring out of plane, 3D STE can track motion of speckles within the scan volume, irrespective of its direction (133). Thus, in addition to strain measurements of longitudinal, radial, and circumferential deformation, as well as combinations of these, rotation and twist parameters can also be quantified. Area strain, which combines the analysis of both longitudinal and circumferential deformations of the LV, offers quantification of endocardial area change (134, 135). In addition, 3D STE can assess a higher proportion of myocardial segments and is able to acquire and analyse 3D dataset (121, 134, 136-140).

1.1.4.2.1 Limitations of three-dimensional speckle tracking echocardiography

Despite the numerous theoretical advantages of 3D STE, it can be limited by image quality and therefore reduced accuracy (141). The relatively low frame rate and spatial resolution of 3D wall motion tracking can also affect the delineation of endocardial and epicardial surfaces and, in turn, the accuracy of tracking (141, 142). Furthermore, stitch artefacts can be inevitable in uncooperative patients and in those with cardiac arrhythmias (141). Similar to earlier work on 2D STE, inter-technique agreement is suboptimal, both for images acquired from different machines and images acquired from the same machine using different software (143).

Functional non-uniformity is found in normal LV in 3D strain measurements where the average value of strain differed significantly between individual segments as well as between different walls and levels of the LV (130). In general, normal values of circumferential and area strains were most consistent with only marginally differences found between different segments, walls, and levels in healthy volunteers while global strain has the best reproducibility as compared to segmental strain measurements (130). Therefore,

choosing a robust 3D strain parameter for clinical practice can be another challenge and may affect the validity of segmental strain assessment.

1.1.4.3 Two-dimensional versus three-dimensional speckle-tracking echocardiography

The comparison between 2D and 3D strains has been challenging for various reasons, (1) the inherent technical issues underlying these 2 imaging modalities as previously mentioned, (2) the wide range of normal strain values with some overlap between physiological and pathological states, (3) the use of global versus segmental strain in terms of feasibility and reproducibility, and (4) the current conflicting literatures which is mainly limited by small study cohorts and significant heterogeneity between studies.

It is still unclear which modalities is better despite 3D imaging's theoretical advantages.

1.1.4.3.1 Strain parameters in two-dimensional and three-dimensional speckle-tracking echocardiography

Global longitudinal strain (GLS) has been shown to be the most robust of the deformation markers, reflecting the favourable effect of averaging when individual measurements are subjected to noise (124). The other advantages of using GLS include (i) images obtained in the axial plane have superior resolution; (ii) there is a greater amount of myocardial tissue in the apical long axis than in the short-axis view of the non-hypertrophied heart (129).

Though a few studies have found that 2D GLS is comparable to 3D GLS in different cohort of patients with varying LV function from preserved LV function (136) to moderate-severe LV dysfunction (126, 144, 145), it is more widely recognized that these two are not interchangeable (137, 146-149). LS and radial strain (RS) by 3D STE are significantly

smaller than by 2D STE, whereas circumferential strain (CS) is significantly larger using 3D STE (139).

1.1.4.3.2 Determinants of strain

Strain parameters are influenced by both patient (age, gender, race, ethnicity, anthropometric), haemodynamic (heart rate, blood pressure), and cardiac factors (LV size, wall thickness) (150). In addition, hypertension (151, 152), diabetes mellitus (153, 154), dialysis (155) and CAD (156) affect strain (129). These factors may act as potential confounders when interpreting the literature on STE especially when some of these co-morbidities commonly co-exist.

1.1.4.4 Speckle-tracking echocardiography in coronary artery disease

Obstructive CAD has been shown to cause subclinical LV dysfunction despite preservation of conventional indices of systolic LV function and no overt infarction (156). This could be secondary to small vessel microembolisation, endothelial dysfunction, or chronic ischaemia (157).

Consistently, 2D GLS has been shown to predict the presence of significant CAD (89, 158-169). In addition, 2D GLS declines incrementally with increasing severity of CAD defined by increasing number of stenotic coronary vessels (162, 163). It may also increase the diagnostic accuracy and sensitivity of stress echocardiography and complements conventional wall motion assessment (158, 163). Interestingly, 2D GLS measurement during stress echocardiography resulted in better diagnostic accuracy for CAD than their resting values (167, 169).

Conversely, Smedsrud and co-authors investigated the predictive value of 2D GLS in detecting significant CAD is only modest in patients with stable chest pain undergoing elective coronary angiography (164). This is further supported by a large prospective multicenter study demonstrating considerable overlap in the distribution of 2D GLS between those with and without acute coronary syndrome (170). A recent metaanalysis revealed similar conclusion (171). This could partly be explained by the fact that CAD is a primarily a regional problem and GLS is a global assessment of LV (171). Previously regional LS has shown greater potential in detecting CAD (172) but its use remains a challenge due to the heterogeneity in obtaining regional strain data (171).

The use of 3D STE in diagnosing and managing patients with CAD is also challenged by inconsistency in the literature in terms of defining the severity of CAD and degree of LV impairment in the study population, as well as the choice of strain measurements.

In patients with LV regional wall abnormalities, AS has been shown to correlate well with LV EF and wall motion score index in a heterogeneous group of patients with different cardiac conditions including CAD (173). Additionally, regional strain by 3D STE is superior to 2D STE for detecting transmural scar in those with ischaemic cardiomyopathy (144). Regional LS by 3D STE, not 2D STE decreases early when the transmural scar is <25% whereas regional RS by 3D STE is decreased only when transmural scar is full thickness. This is consistent with findings from Altman and co-workers where 3D global and regional strain predicted recovery of LV EF after ST-elevation myocardial infarction (134).

In patients with preserved LV EF, Li and coworkers demonstrated 3D multidirectional strain is predictive of moderate and severe CAD (174). Conversely, Sun and coworkers did not find 3D multidirectional peak strains diagnostic of early CAD in the cohort of patients

with chest pain (175). Instead, they found that a composite measurement of peak LS and time to peak LS was predictive of significant CAD (175).

Only one study has compared 2D and 3D strain in patients with CAD. There is a good correlation between 2D GLS and 3D multidirectional strain in patients undergoing percutaneous coronary intervention (176). To date, the role of 2D versus 3D strain in patients with non-obstructive CAD and their predictive values remain uncertain.

1.1.5 Discussion

There are gaps in current literature with regards to the role of EAT and non-obstructive CAD in myocardial dysfunction. First, although there is an association between EAT and the subsequent development of cardiac dysfunction, the published studies included small number of patients with multiple cardiovascular risks factors including obstructive CAD, hypertension and diabetes which could have confounded the results. Secondly, the different methods for EAT quantification with variable reproducibility has been flagged as a major issue. Lastly, although 2D STE is a widely used tool in the quantification of myocardial function, 3D STE is still at its infancy. Further work needs to be done to evaluate the role of 3D STE in identifying subclinical myocardial dysfunction and how it is comparable to its 2D STE in patients with non-obstructive CAD and their values in predicting CAD.

CHAPTER TWO

Aims and hypotheses of research

2.1 Aims

1. Investigate the association between EAT and myocardial function using 3D STE in patients with non-obstructive CAD.
2. The comparison of 2D versus 3D STE in patients without obstructive CAD, diabetes and hypertension.

2.2 Hypotheses

1. EAT is an independent determinant of myocardial function independent of non-obstructive CAD and other cardiovascular risk factors.
2. 3D STE is superior to 2D STE in predicting presence of coronary atherosclerosis in patients without obstructive CAD, diabetes and hypertension.

Publication has been included in chapter three as previously stated (refer to page 6). I have a major role in the conception and design of this study, collection of research data, the analysis and interpretation of the research data on which the publication is based and co-wrote the publication as a joint first author in conjunction with my principal advisor.

CHAPTER THREE

The association of epicardial adipose tissue and subclinical myocardial dysfunction using three-dimensional speckle tracking echocardiography in patients with non-obstructive coronary artery disease

3.1 Aims

We aimed to identify independent determinants of EAT on cardiac CT in patients with non-obstructive CAD, and evaluate the association between EAT and myocardial function using 3D STE multidirectional global strain analysis.

3.2 Methods

3.2.1 Patient population and study protocol

130 patients who presented with low risk chest pain to a tertiary hospital were prospectively recruited to undergo contrast-enhanced cardiac CT and 3D echocardiography. Contrast-enhanced cardiac CT was used to assess for the presence and severity of coronary atherosclerosis as well as to quantify EAT volume (see below). 3D echocardiographic examination included quantifications of 3D LV mass index, end-diastolic volume index (EDVI), end-systolic volume index (ESVI), LV EF and 3D multidirectional global strain [including GLS, global circumferential strain (GSC), global radial strain (GRS) and global area strain (GAS)].

Exclusion criteria in the present study included LV EF <50% or previous cardiomyopathies or heart failure, moderate or severe valvular heart disease, congenital heart disease, previous history of CAD, obstructive CAD on contrast-enhanced cardiac CT defined as >50% coronary stenosis, atrial fibrillation and contraindications for cardiac CT examination. Contraindications for cardiac CT examination included supraventricular or ventricular arrhythmias, renal insufficiency defined as a glomerular filtration rate < 30 mL/min/1.73m^2, known iodine contrast allergy, severe claustrophobia, and pregnancy. In 6 patients with intermediate CAD stenosis (i.e. 50% stenosis), ischaemia was excluded by stress echocardiography (n = 5) or stress technetium-99m sestamibi myocardial perfusion scan (n = 1).

The mean and median dose-length product for the cardiac CT examination (including calcium scoring and contrast-enhanced CT coronary angiography) were 368.2 ± 302.6 mGy.cm and 313.0 mGy.cm (25th and 75th percentile, 164.0 and 490.0 mGy.cm) respectively. Using a conversion factor of 0.014 for chest CT in adults (177), the mean and median estimated effective radiation dose were 5.2 ± 4.2 mSv and 4.4 mSv (25th and 75th percentile, 2.3 and 6.9 mSv) respectively.

The median time difference between cardiac CT and echocardiography was 1.0 month (25th and 75th percentile, 0.4 and 1.7 months).

The study was approved by the institutional ethics committee.

3.2.2 Cardiac CT data acquisition

All patients underwent cardiac CT using a dual-source CT system (Somatom Definition Flash, Siemens Healthcare, Forchheim, Germany). Cardiac CT was acquired using prospective ECG gating triggered at 60% of the R-R interval, with a collimation of 2 x 128 x 0.6mm and a gantry rotation time of 280ms. The tube current was 80mA.s and tube voltage

was 100 kV or 120 kV as determined by patient's BMI. From the raw data, cross-sectional images were reconstructed with 0.75mm slice thickness and a soft reconstruction kernel (Siemens B26f).

Patient's heart rate and blood pressure were monitored prior to each scan and beta-blockers (25 to 100mg Metoprolol orally) were administered in the absence of contraindications. All scans were performed during mid-inspiratory breath-hold and 75 mL of Ioversol (Optiray 350, Mallinckrodt Medical, St. Louis, MO) was injected into the antecubital vein. All cardiac CT images were subsequently exported to dedicated workstations (SyngoVia, Siemens Healthcare, Forchheim, Germany; MASS V2010-EXP, Leiden University Medical Center, Leiden, The Netherlands) for off-line post-processing.

3.2.3 Epicardial adipose tissue quantification

For EAT volume quantification, the pericardium was manually traced on every single cross-sectional image, starting from the level of the pulmonary artery bifurcation to the level of the diaphragm (Figure 1). Within these contour limits, a CT attenuation threshold of -50 to -200 Hounsfield Unit was used to isolate EAT as previously published (99, 178). Mediastinal fat and pericardial fat (outside the visceral pericardium and on the external surface of the parietal pericardium) were excluded.

Figure 1. Quantification of epicardial adipose tissue on cardiac CT.

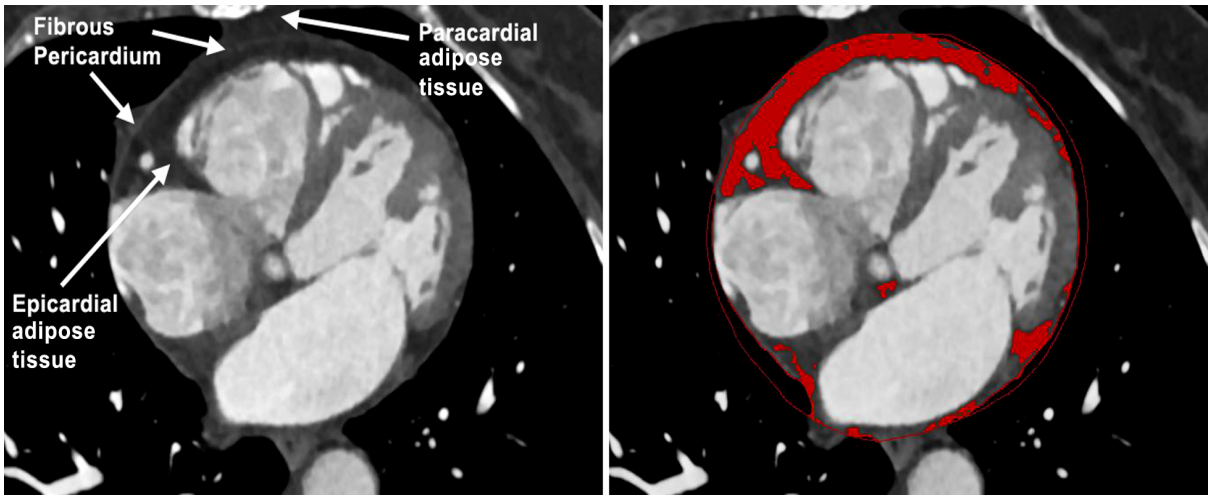

Epicardial adipose tissue is defined as fat between the heart and the fibrous pericardium, whereas paracardial adipose tissue is external to the pericardium (left panel). Contours were drawn along the pericardium and epicardial adipose tissue is automatically identified by the software (red colour) (right panel).

3.2.4 Echocardiography

Transthoracic echocardiography was performed with the subjects at rest using a commercially available ultrasound system (Vivid E9, 4V probe, GE-Vingmed, Horten, Norway). A complete 2D, 3D, colour, pulsed and continuous-wave Doppler echocardiogram was performed (179, 180). Image contrast, depth and sector size were optimized during image acquisition, with care taken to avoid foreshortened views, to include the entire myocardial wall, and an optimal frame rate of > 30 frames per second. Images were obtained during breath-hold to achieve a multi-beat 3D volume of a minimum of 4 heartbeats without artifacts (Figure 2). All images were digitally stored on hard disks for offline analysis. 3D LV mass index, LV EDVI, and LV ESVI were calculated using the 3D dataset and corrected for body surface area (181). LV EF was calculated and expressed as a percentage.

3.2.4.1 Three-dimensional speckle tracking echocardiography

3D multidirectional global strains were calculated from the 3D dataset using commercially available software (4D Auto LVQ, EchoPAC version 113, GE-Vingmed, Horten, Norway). Briefly, 3D volume datasets were initially displayed as conventional apical and short axis views (Figure 2). Automatic LV border contours were created after placing 2 points, one at the center of the LV base and the other at the apex, in the end-diastolic and end-systolic apical views. The LV epicardial and endocardial border contours were adjusted if required. The motion of the 3D myocardium was subsequently tracked automatically throughout the entire cardiac cycle and myocardial deformation was calculated for each segmental volume. A multidirectional 17 segments Bull's eye map with 3D GLS, GCS, GRS and GAS results were finally generated and displayed.

Figure 2. A representative graphical display of EAT volumes traced on CT and speckle tracking on 3D echocardiography for 2 patients.

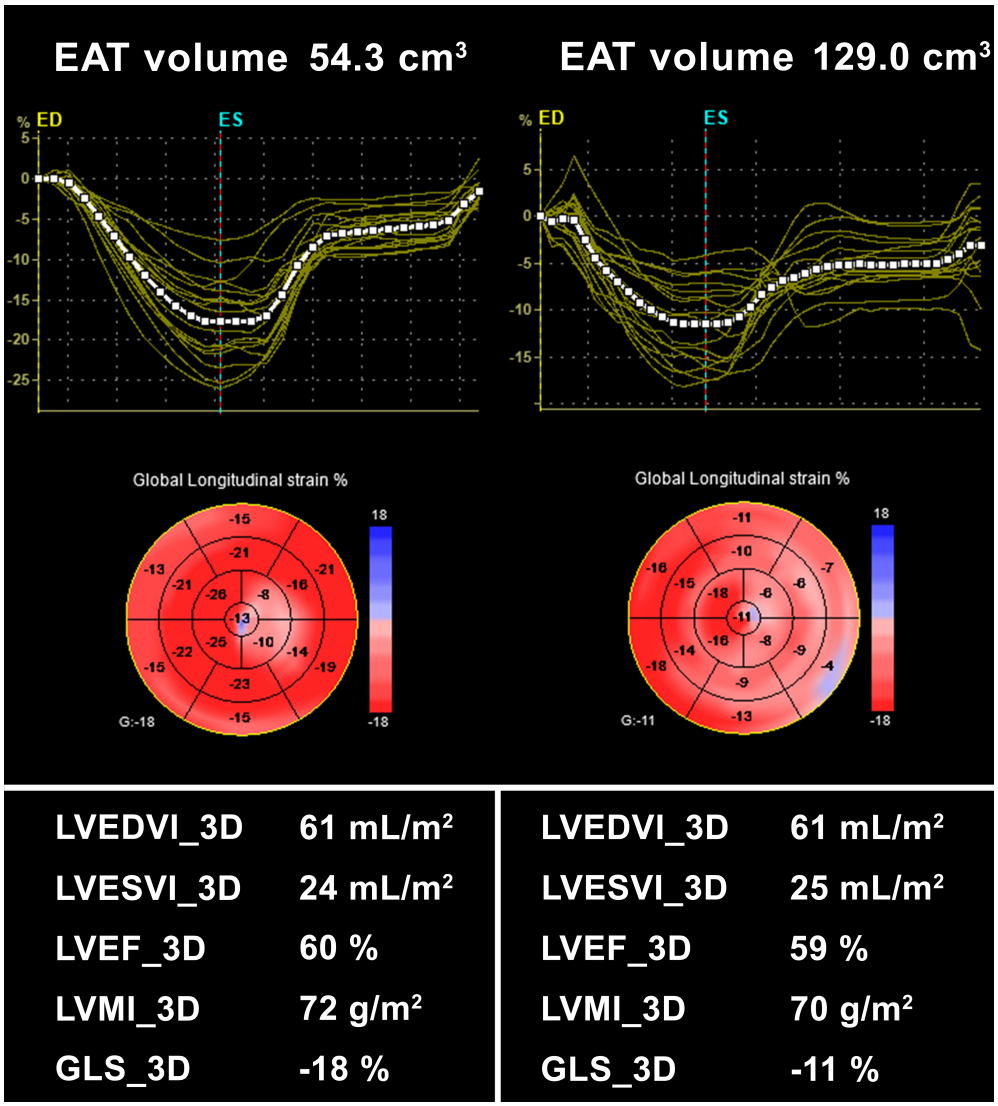

Examples of 3D STE in 2 female patients with 54.3cm^3 and 129.0cm^3 of epicardial adipose tissue respectively. Both patients had comparable LV mass index, volumes and EF, but 3D GLS was significantly more impaired in the patient with larger epicardial adipose tissue volume.

3D: 3-dimensional; EAT: epicardial adipose tissue; EDVI: end-diastolic volume index; ESVI: end-systolic volume index; EF: ejection fraction; GLS: global longitudinal strain; LV: left ventricular; LVMI: left ventricular mass index.

3.2.5 Statistical Analysis

All continuous variables were tested for Gaussian distribution. Continuous variables were presented as mean ± 1 standard deviation unless otherwise stated. Categorical variables were presented as frequencies and percentages, and were compared using Chi-square test when all expected cell counts were ≥ 5, or Fisher's exact test if expected cell count was < 5. Unpaired Student's t-test was used to compare 2 groups of continuous variables of Gaussian distribution. Pearson correlation was used to determine the association between 2 continuous variables. Multiple linear regression analyses were performed to identify independent determinants of both EAT volume and 3D multidirectional GLS, GCS, GRS and GAS with significant univariable determinants entered simultaneously as covariates. To avoid multicollinearity, a tolerance of > 0.4 (equating to a Variance Inflation Factor of > 2.5) was set. As the presence of diabetes, hypertension and non-obstructive coronary atherosclerosis may potentially confound the multidirectional global strain analyses, these variables were forced into all the multivariable models. In addition, to further confirm the study results, all multivariable analyses were repeated in patients without diabetes, hypertension and coronary atherosclerosis. Similarly, all analyses were repeated in patients with BMI ≤ 25.0 kg/m^2 to exclude suboptimal image quality due to obesity as a confounding factor in artificially reducing the 3D multidirectional global strain measurements. In 10 randomly selected subjects, intra- and inter-observer measurement variabilities for EAT volume and 3D multidirectional global strain were presented as mean absolute differences. A 2-tailed p value of < 0.05 was considered significant. All statistical analyses were performed using IBM SPSS Statistics, version 21.0 (Armonk, NY).

3.3 Results

Table 1 outlines the baseline clinical, cardiac CT and echocardiographic characteristics for all the patients. The mean age was 53 ± 9 years, 53.1% male. Men were younger (50 ± 9 vs. 56 ± 8 years, $p < 0.001$) had significantly higher waist/hip ratio (0.97 ± 0.06 vs. 0.89 ± 0.06, $p < 0.001$), and less likely to have a history of hypertension ($p = 0.01$).

The mean EAT volume on cardiac CT was 97.5 ± 43.7 cm^3 (range 20.0 – 235.2 cm^3). Although there was a trend towards larger EAT volume in men (103.7 ± 39.5 vs. 90.4 ± 47.4 cm^3, $p = 0.08$), and there were no gender differences in the presence or absence of coronary atherosclerosis ($p = 0.19$) or Agatston calcium score (56.2 ± 130.2 vs. 34.6 ± 109.7, $p = 0.31$).

Patients with evidence of coronary atherosclerosis had significantly larger EAT volume (107.4 ± 44.9 vs. 84.4 ± 38.8 cm^3, $p = 0.003$). However, there was no correlation between EAT volume and Agatston calcium score ($r = 0.089$, $p = 0.32$).

Finally, on 3D echocardiography, men had significantly larger LV volumes and lower 3D multidirectional global strain (Table 1). Although there was a gender difference in LV EF, all patients had normal LV EF.

Table 1. Baseline clinical, cardiac computed tomography and echocardiographic characteristics

Variable	Total population (n = 130)	Male (n = 69)	Female (n = 61)	p value
Clinical				
Age (years)	53 ± 9	50 ± 9	56 ± 8	< 0.001
Body mass index (kg/m^2)	28.2 ± 5.3	27.8 ± 5.4	28.6 ± 5.3	0.38

Waist/hip ratio	0.93 ± 0.07	0.97 ± 0.06	0.89 ± 0.06	< 0.001
Hypertension (%)	30.0	20.3	41.0	0.010
Diabetes (%)	10.0	11.6	8.2	0.52
Hypercholesterolemia (%)	36.9	34.8	39.3	0.59
Heart rate (beats/min)	70 ± 11	69 ±10	71 ± 12	0.27
Systolic BP (mmHg)	133 ± 16	132 ± 15	134 ± 18	0.43
Diastolic BP (mmHg)	81 ± 10	81 ± 9	81 ± 12	0.77
Cardiac CT				
Presence of coronary atherosclerosis (%)	56.9	62.3	50.8	0.19
Agatston calcium score	46.1 ± 121.0	56.2 ± 130.2	34.6 ± 109.7	0.31
Epicardial adipose tissue volume (cm^3)	97.5 ± 43.7	103.7 ± 39.5	90.9 ± 47.4	0.08
3D Echocardiography				
LV mass index (g/m^2)	72.4 ± 9.3	72.9 ± 8.8	71.8 ± 9.7	0.51
LV EDVI (mL/m^2)	57.2 ± 10.6	60.2 ± 10.6	53.9 ± 9.7	0.001
LV ESVI (mL/m^2)	23.2 ± 5.1	25.0 ± 4.8	21.2 ± 4.6	< 0.001
LV EF (%)	59.5 ± 4.7	58.4 ± 4.5	60.8 ± 4.5	0.003
Global longitudinal strain (%)	-15.4 ± 3.2	-14.5 ± 2.9	-16.4 ± 3.3	0.001
Global circumferential strain (%)	-16.2 ± 3.4	-15.8 ± 3.2	-16.5 ± 3.5	0.23

Global radial strain (%)	42.1 ± 10.5	40.0 ± 9.5	44.4 ± 11.2	0.016
Global area strain (%)	-28.0 ± 5.0	-27.0 ± 4.7	-29.1 ± 5.1	0.017

3D: 3-dimensional; BP: blood pressure; CT: computed tomography; EDVI: end-diastolic volume index; ESVI: end-systolic volume index; EF: ejection fraction; LV: left ventricular

3.3.1 Determinants of epicardial adipose tissue volume

To identify independent determinants of EAT volume, all significant univariable determinants (BMI, waist/hip ratio and systolic blood pressure) were simultaneously entered into a multiple linear regression model. Table 2 shows that only measures of obesity (BMI [standardized $\beta = 0.230$, $p = 0.007$] and waist/hip ratio [standardized $\beta = 0.266$, $p = 0.001$]) were independently associated with larger EAT volume.

Table 2. Univariable and multivariable linear regression models for epicardial adipose tissue volume

	Univariable		Multivariable	
Variable	Standardized β	p value	Standardized β	p value
BMI	0.382	< 0.001	0.230	0.007
Waist/hip ratio	0.359	< 0.001	0.266	0.001
Systolic BP	0.305	< 0.001	0.129	0.18
Diastolic BP	0.316	< 0.001	0.131	0.17

BMI: body mass index; BP: blood pressure

3.3.2 Determinants of three-dimensional multidirectional global strain

Table 3 summarizes all the univariable and multivariable determinants of 3D GLS. On univariable analysis, patients with coronary atherosclerosis had significantly lower 3D

GLS (-14.9 ± 3.1 vs. -16.1 ± 3.2%, p = 0.041). However, there was a non-significant association between 3D GLS and Agatston calcium score (r = 0.125, p = 0.16). Figure 3 shows the correlation between EAT volume and 3D GLS.

Table 3. Univariable and multivariable linear regression models for 3-dimensional global longitudinal strain

	Univariable		Multivariable	
	Standardized β	p value	Standardized β	p value
Male gender	0.294	0.001	0.114	0.23
Hypertension	0.180	0.040	0.115	0.14
Diabetes	0.164	0.06	0.080	0.26
BMI	0.215	0.014	-0.108	0.17
Waist/hip ratio	0.361	< 0.001	0.080	0.38
Systolic BP	0.324	< 0.001	0.064	0.46
Diastolic BP	0.298	0.001	0.078	0.34
LV ESVI	0.350	< 0.001	0.213	0.008
Presence of coronary atherosclerosis	0.179	0.041	-0.016	0.83
Epicardial adipose tissue volume	0.601	< 0.001	0.512	< 0.001

BMI: body mass index; BP: blood pressure; ESVI: end-systolic volume index; LV: left ventricular.

Figure 3. Correlation between epicardial adipose tissue volume and 3D global longitudinal strain. Patients with larger epicardial adipose tissue volume have significantly more impaired myocardial function despite a preserved LV EF. 3D: 3-dimensional.

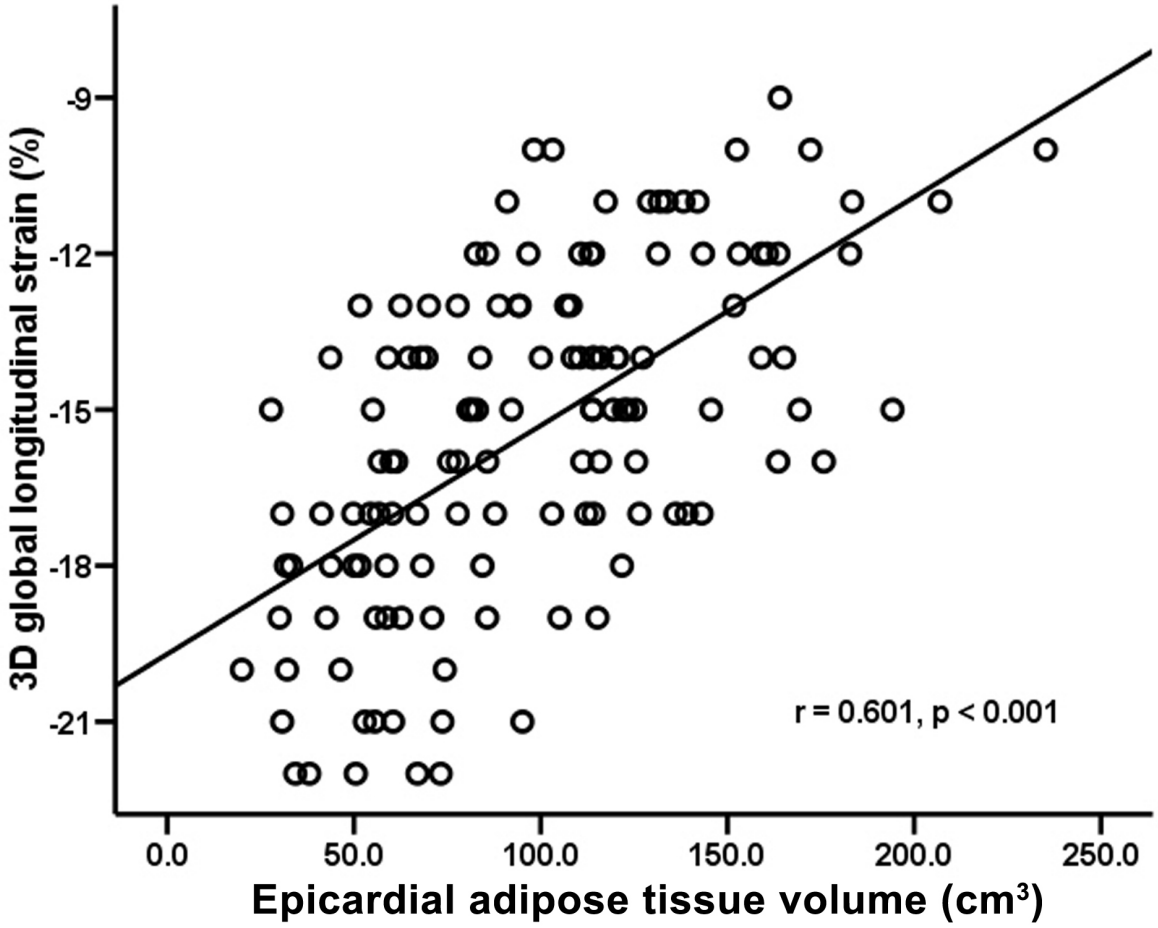

Potential confounders of 3D GLS such as presence of diabetes, hypertension and non-obstructive CAD were included into the multivariable analysis. Only EAT volume (standardized $\beta = 0.512$, $p < 0.001$) and LV ESVI (standardized $\beta = 0.213$, $p = 0.008$) were independent determinants of 3D GLS (Table 3). Based on the standardized β, EAT volume was the strongest predictor of 3D GLS. Similarly, EAT volume was an independent determinant of 3D GCS (Table 4), GRS (Table 5) and GAS (Table 6).

Table 4. Univariable and multivariable linear regression models for 3-dimensional global circumferential strain

	Univariable		Multivariable	
	Standardized β	p value	Standardized β	p value
Hypertension	0.299	0.001	0.243	0.003
Diabetes	0.228	0.009	0.090	0.25
BMI	0.283	0.001	-0.011	0.90
Waist/hip ratio	0.271	0.002	0.102	0.21
Systolic BP	0.230	0.009	-0.072	0.43
Diastolic BP	0.233	0.008	0.107	0.23
LV mass index	-0.194	0.027	-0.179	0.024
LV ESVI	0.429	< 0.001	0.350	< 0.001
Presence of coronary atherosclerosis	0.055	0.54	-0.061	0.42
EAT volume	0.375	< 0.001	0.242	0.006

BMI: body mass index; BP: blood pressure; EAT: epicardial adipose tissue; ESVI: end-systolic volume index; LV: left ventricular.

Table 5. Univariable and multivariable linear regression models for 3-dimensional global radial strain

	Univariable		Multivariable	
	Standardized β	p value	Standardized β	p value
Male gender	-0.211	0.016	0.020	0.83
Hypertension	-0.245	0.005	-0.179	0.022
Diabetes	-0.220	0.012	-0.088	0.22

BMI	-0.296	0.001	0.070	0.39
Waist/hip ratio	-0.353	< 0.001	-0.149	0.10
Systolic BP	-0.283	0.001	0.041	0.63
Diastolic BP	-0.297	0.001	-0.126	0.12
LV mass index	0.186	0.034	0.166	0.024
LVESVI	-0.393	< 0.001	-0.312	< 0.001
Presence of coronary atherosclerosis	-0.115	0.19	0.051	0.47
EAT volume	-0.546	< 0.001	-0.422	< 0.001

BMI: body mass index; BP: blood pressure; EAT: epicardial adipose tissue; ESVI: end-systolic volume index; LV: left ventricular.

Table 6. Univariable and multivariable linear regression models for 3-dimensional global area strain

	Univariable		Multivariable	
	Standardized β	p value	Standardized β	p value
Male gender	0.209	0.017	0.006	0.95
Hypertension	0.252	0.004	0.179	0.022
Diabetes	0.221	0.011	0.087	0.23
BMI	0.308	< 0.001	-0.053	0.52
Waist/hip ratio	0.341	< 0.001	0.116	0.20
Systolic BP	0.289	0.001	-0.032	0.71
Diastolic BP	0.302	< 0.001	0.123	0.13
LV mass index	-0.206	0.019	-0.174	0.018
LV ESVI	0.374	< 0.001	0.284	< 0.001

Presence of coronary atherosclerosis	0.133	0.13	-0.027	0.70
EAT volume	0.558	< 0.001	0.428	< 0.001

BMI: body mass index; BP: blood pressure; EAT: epicardial adipose tissue; ESVI: end-systolic volume index; LV: left ventricular.

3.3.3 Subgroup analyses

A subgroup analysis was performed in 39 patients without diabetes, hypertension and any coronary atherosclerosis on cardiac CT as these co-morbidities could affect strain. Similarly, EAT volume was significantly correlated with 3D GLS ($r = 0.538$, $p < 0.001$), GCS ($r = 0.421$, $p = 0.008$), GRS ($r = -0.579$, $p < 0.001$), and GAS ($r = 0.582$, $p < 0.001$). On multivariable analyses, EAT volume was an independent determinant of 3D GLS (standardized $\beta = 0.398$, $p = 0.008$). Although not significant, larger EAT volume trended towards lower 3D GCS (standardized $\beta = 0.126$, $p = 0.51$), GRS (standardized $\beta = -0.341$, $p = 0.076$), and GAS (standardized $\beta = 0.345$, $p = 0.070$).

Another subgroup analysis was performed in 40 patients with BMI ≤ 25.0 kg/m^2 as obesity can affect image quality and the accuracy of strain measurements. Similarly, EAT volume was significantly correlated with 3D GLS ($r = 0.668$, $p < 0.001$), GCS ($r = 0.499$, $p = 0.001$), GRS ($r = -0.618$, $p < 0.001$), and GAS ($r = 0.629$, $p < 0.001$). On multivariable analyses, EAT volume was an independent determinant of 3D GLS (standardized $\beta = 0.414$, $p = 0.006$), GRS (standardized $\beta = -0.547$, $p = 0.006$), and GAS (standardized $\beta = 0.575$, $p = 0.003$). There was also a trend for larger EAT volume and more impaired 3D GCS (standardized $\beta = 0.215$, $p = 0.21$).

Finally, increased EAT volume may have a direct mechanistic effect on 3D multidirectional global strain by "constricting" LV systolic and diastolic volumes. However,

there were no correlations between EAT volume and LV EDVI (r = -0.09, p = 0.29) or LV ESVI (r = 0.08, p = 0.35). Furthermore, unlike pericardial constriction, early diastolic velocities (E^1) by tissue Doppler imaging are usually preserved or even supranormal, there were inverse relationships between EAT volume and septal E^1 (r = -0.263, p = 0.002) and lateral E^1 velocities (r = -0.285, p = 0.001). Therefore, increased EAT volume was unlikely to impair 3D multidirectional global strain by physically "constricting" LV systole and diastole.

3.3.4 Measurement variabilities

Table 7 outlines the intra- and interobserver measurement variabilities for EAT volume and 3D multidirectional global strain analyses.

Table 7. Intraobserver and interobserver measurement variabilities for epicardial adipose tissue volume and 3-dimensional multidirectional global strain

Variable	Intraobserver Absolute Difference	Interobserver Absolute Difference
EAT volume (cm^3)	0.9 ± 1.0	1.7 ± 1.7
3D global longitudinal strain (%)	1.3 ± 1.3	2.0 ± 1.6
3D global circumferential strain (%)	3.4 ± 2.3	3.7 ± 2.3
3D global radial strain (%)	8.3 ± 5.9	9.2 ± 6.6
3D global area strain (%)	3.8 ± 2.8	4.3 ± 3.3

EAT: epicardial adipose tissue; 3D: 3-dimensional

3.4 Discussion

The present study sought to determine the association between EAT volume and myocardial function using 3D multidirectional global strain. To our knowledge, the present

study was the first to demonstrate that increased EAT volume was independently associated with lower 3D multidirectional global strain in patients with low risk chest pain and preserved LV EF. Even though other measures of obesity (defined as increased BMI or waist/hip ratio) were independently associated with larger EAT volume, only EAT volume was associated with impaired LV strain. In addition, the association between EAT volume and LV strain was independent of other confounders of strain such as coronary atherosclerosis, hypertension, diabetes or image quality. Finally, the observed association between EAT and myocardial contractile function was likely secondary to EAT and its role in myocardial lipid and energy homeostasis, steatosis and lipotoxicity, rather than a direct mechanistic effect in physically "constricting" LV systole and diastole.

3.4.1 Epicardial adipose tissues and coronary artery disease

Consistent with current literature (61, 178), this present study demonstrated that patients with coronary atherosclerosis had significantly larger EAT volume. However, the present study is the first to demonstrate an inverse relationship between EAT volume and myocardial contractile function.

One of the major strength of the present study was the exclusion of significant CAD as a potential confounding factor that could have impaired myocardial contractility. This was confirmed with the subgroup analysis where EAT was still associated with impaired LV strain in patients without any coronary atherosclerosis on the contrast-enhanced cardiac CT. This highlights the pathophysiological role of EAT on myocardium independent of its effect on coronary atherosclerosis.

3.4.2 Epicardial adipose tissue, myocardial steatosis and contractile dysfunction

Diabetes and obesity can lead to extra cardiac and intramyocardial TG accumulation (i.e. steatosis) under conditions of excess free fatty acids (87, 95). These excess fatty acids could directly diffuse from EAT to myocardium and these are shunted into non-oxidative pathways and lead to accumulation of toxic intermediates such as diacylglycerol and ceramide that disrupt cellular signaling and cause apoptosis, fibrosis and myocardial contractile dysfunction (7, 15, 87, 94, 95).

Although previous studies have shown that increased EAT was associated with increased LV mass and diastolic dysfunction (80, 84, 182), this present study demonstrated an inverse independent relationship between EAT and myocardial contractility. Even when patients with diabetes, hypertension and coronary atherosclerosis were excluded, EAT volume was still an independent determinant of longitudinal myocardial function.

3.4.3 Other potential confounding factors of strain measurement

3D STE is a relatively new imaging modality and it is not directly comparable to 2D STE (148). The feasibility in successfully analyzing 3D myocardial strain is lower (148), and obesity can reduce signal-to-noise ratio and may artificially reduce the absolute strain measurements (183). To reduce the false likelihood that the observed results were secondary to lower signal-to-noise ratio, we repeated all analyses in patients with BMI ≤ 25.0 kg/m^2. The continuing observation of the independent association between EAT volume and 3D multidirectional global strain in patients with normal BMI suggested that poor image quality in obese patients was unlikely to be significant confounding factor.

3.4.4 Study limitations

Although we demonstrated an independent association between EAT volume and impaired 3D multidirectional global strain, it does not imply causality between increased EAT volume and reduced myocardial strain. However, previous in-vitro study has demonstrated that EAT explanted from guinea pigs secrete factors that inhibited isolated cardiomyocyte contractile function and induced insulin resistance (184). Secondly, no comparisons were made between the sensitivity of 2D versus 3D STE in detecting myocardial dysfunction.

3.5 Conclusions

Obesity is known to be associated with myocardial dysfunction and heart failure (185-187). Although the pathophysiology is unclear, visceral adiposity has been proposed to impair myocardial contractility through myocardial steatosis and lipotoxicity as seen in diabetic patients (182, 188). We demonstrated that EAT is associated with subclinical myocardial systolic dysfunction, independent of significant CAD, diabetes and hypertension, and is superior to other measures of obesity such as BMI and waist/hip ratio. Future studies should consider quantification of EAT volume when evaluating LV myocardial function and explore EAT as a potential target for management of patients with metabolic and diabetic heart disease.

CHAPTER FOUR

Comparison of two-dimensional and three-dimensional speckle tracking echocardiography in patients without obstructive coronary artery disease, diabetes or hypertension

4.1 Aims

We aimed to investigate (1) the effect of non-obstructive coronary atherosclerosis on subclinical myocardial systolic dysfunction in patients without diabetes or hypertension using 2D and 3D STE, and (2) compare the sensitivity and clinical usefulness 2D versus 3D STE in detection of non-obstructive CAD.

4.2 Methods

4.2.1 Patient population and study protocol

A total of 96 patients with low risk chest pain who underwent contrast-enhanced cardiac CT imaging and 2D and 3D echocardiographic imaging were included. Non-obstructive CAD on cardiac CT imaging was defined as < 50% coronary stenosis, while no CAD was defined as zero calcium score and absence of any coronary plaques. Exclusion criteria included hypertension, diabetes, LV EF < 50%, previous cardiomyopathies or heart failure, moderate or severe valvular heart disease, congenital heart disease, history of previous myocardial infarction, percutaneous coronary intervention, or coronary artery bypass grafting, obstructive CAD on cardiac CT imaging defined as > 50% coronary stenosis, atrial fibrillation, and contraindications for cardiac CT examination. Contraindications for cardiac CT examination included supraventricular or ventricular arrhythmias, renal insufficiency (glomerular filtration rate <30 mL/min/1.73 m^2), iodine contrast allergy, severe

claustrophobia, and pregnancy. Modification of Diet in Renal disease (MDMR) equation was used to calculate glomerular filtration rate (eGFR) (189).

4.2.2 CT data acquisition

This has been previously described (refer to section 3.2.2).

4.2.3 Echocardiography

This has been previously described (refer to section 3.2.4). The LV mass index, LV EDVI, and LV ESVI were calculated using the 3D dataset and corrected for body surface area.

4.2.3.1 Three-dimensional speckle tracking echocardiography

This has been previously described (refer to section 3.2.4.1).

4.2.3.2 Two-dimensional speckle tracking echocardiography

Peak systolic LS measurements calculated from the 2D data recorded in apical 4-chamber, 2-chamber and long-axis views using commercial available software (EchoPAC version 113, GE-Vingmed, Horten, Norway). After the definition of the LV endocardial border was automatically defined, the endocardium was automatically tracked throughout the cardiac cycle. The software algorithm automatically divided the LV apical view into 6 segments for speckle tracking throughout the cardiac cycle. GLS was obtained from each apical view and averaged (190).

4.2.4 Statistical analysis

All continuous data were presented as mean ± standard deviation. The differences between patients with non-obstructive CAD and without CAD were compared using unpaired Student's t tests or chi-square tests, as appropriate. Multiple logistic regression analysis was used to identify independent associations for the presence or absence of CAD with univariable predictors ($p < 0.10$) entered in a stepwise manner into a multivariate logistic regression model. Comparison of receiver-operating characteristic curve analysis was used to determine the discriminatory value of 2D versus 3D GLS in identifying the presence of coronary atherosclerosis. To further compare the clinical usefulness of 2D versus 3D GLS in identifying the presence of coronary atherosclerosis, decision curve analysis was performed. For all analyses, p values < 0.05 were considered as statistical significant. All statistical analyses were performed using IBM SPSS Statistics, version 21.0 (Armonk, NY), STATA, release 15 (College Station, Texas) and R for stats, version 3.3.2 (Vienna, Austria).

The study was approved by the ethics committee of the participating institution.

4.3 Result

The baseline clinical and echocardiographic characteristics for all the patients are shown in Table 8 and 9. The mean age was 51 ± 8.6 years, 56% male. 50% patients had non-obstructive CAD. Patients with non-obstructive CAD were older (53 ± 8 vs. 49 ± 9 years, $p = 0.02$) with higher resting diastolic blood pressure (81 ± 9 vs. 77 ± 9 mmHg, $p = 0.03$). The CAD patients had a mean Agatston score of 62 ± 112, 56% with 1-vessel disease, 21% with 2-vessels and 23% with 3-vessels disease. There were no differences in other cardiac risk factors including gender, BMI, waist-hip ratio, hypercholesterolaemia, smoking status and family history of CAD between patients with or without coronary atherosclerosis.

Table 8 Demographics and baseline clinical characteristics.

Variables	Total cohort (n = 96)	Patients with CAD (n = 48)	Patients without CAD (n = 48)	p Value
Age, years	51 ± 9	53 ± 8	49 ± 9	0.023
Male, %	56	65	48	0.10
BMI, kg/m^2	28 ± 6	28 ± 6	27 ± 6	0.71
Waist-hip ratio	0.9 ± 0.07	0.9 ± 0.07	0.9 ± 0.07	0.09
Hypercholesterolaemia, %	34	38	31	0.52
Current Smoker, %	31	33	29	0.66
Family history of CAD, %	31	27	35	0.38
Systolic BP, mmHg	129 ± 15	129 ± 15	128 ± 16	0.70
Diastolic BP, mmHg	79 ± 9	81 ± 9	77 ± 9	0.028
Mean arterial BP, mmHg	96 ± 10	97 ± 10	94 ± 19	0.12
Fasting blood glucose, mmol/L	5.6 ± 0.9	5.7 ± 0.8	5.7 ± 0.9	0.91
HBA1c, %	5.6 ± 0.4	5.6 ± 0.8	5.5 ± 0.3	0.52
Total cholesterol, mmol/L	5.1 ± 1.2	5.3 ± 1.3	4.9 ± 0.9	0.13
LDL cholesterol, mmol/L	3.1 ± 1.1	3.2 ± 1.4	3.0 ± 0.8	0.40

HDL cholesterol, mmol/L	1.3 ± 0.3	1.3 ± 0.4	1.2 ± 0.3	0.38
Triglyceride, mmol/L	1.5 ± 0.9	1.6 ± 1.0	1.5 ± 0.9	0.55
Creatinine, µmol/L	73 ± 16	76 ± 16	70 ± 15	0.08
eGFR, mL/min/1.73 m^2	51 ± 10	50 ± 8	53 ± 11	0.09

BMI: body mass index, BP: blood pressure, CAD: coronary artery disease, HBA1c: glycated haemoglobin, eGFR: glomerular filtration rate, HDL: high density lipoprotein, LDL: low density lipoprotein.

The mean 2D GLS was -19.3 ± 2.2% and the mean 3D GLS was -15.6 ± 2.8%. Compared to those without CAD, the 2D and 3D GLS were lower in those with coronary atherosclerosis (-18.5 ± 2.2% vs. -20.1 ± 1.9%, $p < 0.001$; -14.9 ± 2.4% vs. -16.3 ± 3.1%, $p = 0.01$). There was no difference in average E/e^1 ratio and other multidirectional 3D strain measurements (GCS, GRS and GAS) between the two groups.

Table 9 Baseline two-dimensional and three-dimensional echocardiographic characteristics.

Echocardiographic Variables	Total cohort (n = 96)	Patients with CAD (n = 48)	Patients without CAD (n = 48)	p Value
3D-LV EDVI, ml/m2	57 ± 10	56 ± 10	58 ± 10	0.30
3D-LV ESVI, ml/m2	23 ± 5	23 ± 4	23 ± 5	0.10
LV EF, %	59 ± 5	58 ± 5	60 ± 5	0.051
3D-LV mass indexed, g/m2	73 ± 9	73 ± 10	72 ± 8	0.41
Mitral E wave, m/s	0.6 ± 0.2	0.6 ± 0.2	0.7 ± 0.2	0.009
Mitral A wave, m/s	0.6 ± 0.2	0.6 ± 0.1	0.6 ± 0.2	0.67
Transmitral E/A ratio	1.1 ± 0.3	1.0 ± 0.3	1.2 ± 0.4	0.027
Mitral deceleration time, msec	197 ± 41	204 ± 40	191 ± 41	0.14
Average E/e' ratio	7.7 ± 2.3	7.7 ±1.9	7.7 ± 2.6	0.19
2D-Global longitudinal strain, %	-19.3 ± 2.2	-18.5 ± 2.2	-20.1 ± 1.9	<0.001
3D-Global longitudinal strain, %	-15.6 ± 2.8	-14.9 ± 2.4	-16.3 ± 3.1	0.011
3D-Global circumferential strain, %	-16.2 ± 3.3	-16.1 ± 3.2	-16.4 ± 3.4	0.67

3D-Global radial strain, %	42.4 ± 9.5	41.3 ± 8.6	43.5 ± 10.3	0.24
3D-Global area strain, %	-28.2 ± 4.6	-27.6 ± 4.1	-29.0 ± 5.1	0.18

EF: ejection fraction, EDVI: Indexed end diastolic volume, ESVI: Indexed end diastolic volume, LV: left ventricular.

4.3.1 Predictors of coronary atherosclerosis

To determine the predictors of coronary atherosclerosis, we performed univariate and multivariate analysis of association between baseline clinical and echocardiographic variables and coronary atherosclerosis. In the multivariable logistic regression model using 2D GLS, both age and 2D GLS were associated with coronary atherosclerosis (Table 10). Similarly, in a separate multivariate model using 3D GLS, both age and 3D GLS were associated with coronary atherosclerosis (Table 11).

Table 10 Univariable and multivariable logistic regression analysis of association of two-dimensional echocardiographic variables with non-obstructive coronary artery disease.

Variables	Univariable analysis		Multivariable analysis	
	OR (95% CI)	p Value	OR (95% CI)	p value
Age (per decade increase)	1.78 (1.07-2.95)	0.026	2.16 (1.20-3.90)	0.011
eGFR, mL/min/1.73 m^2	0.98 (0.96-1.00)	0.089		

Waist-hip ratio (per 0.1 increase)	1.63 (0.91-2.93)	0.099		
Transmitral E/A ratio	0.25 (0.07-0.89)	0.032		
2D-Global longitudinal strain,%	1.45 (1.17-1.80)	0.001	1.55 (1.20-2.01)	0.001

BP: blood pressure, CAD: coronary artery disease, CI: confidence interval, 2D: two-dimensional, eGFR: glomerular filtration rate, OR: odd ratio

Table 11 Univariable and multivariate logistic regression analysis of association of three-dimensional echocardiographic variables with non-obstructive coronary artery disease.

Variables	Univariable analysis		Multivariable analysis	
	OR (95% CI)	p Value	OR (95% CI)	p value
Age (per decade increase)	1.78 (1.07-2.95)	0.026	2.23 (1.25-4.01)	0.007
eGFR, mL/min/1.73 m^2	0.98 (0.96-1.00)	0.089		
Waist-hip ratio (per 0.1 increase)	1.63 (0.91-2.93)	0.099		
Transmitral E/A ratio	0.25 (0.07-0.89)	0.032		
3D-Global longitudinal strain, %	1.22 (1.04-1.42)	0.014	1.21 (1.02-1.43)	0.027

BP: blood pressure, CAD: coronary artery disease, CI: confidence interval, 3D: three-dimensional, eGFR: glomerular filtration rate; OR: odd ratio

Based on the receiver operating characteristic curve analysis, 2D GLS has higher area under the curve (0.70; p = 0.001) compared to 3D GLS (0.65; p = 0.01). However, there is no

significant difference between the area under the curve of 2D and 3D GLS (p = 0.44) in predicting non-obstructive coronary atherosclerosis.

4.3.2 Decision Curve Analysis

To evaluate and compare the clinical usefulness of 2D GLS versus 3D GLS in identifying coronary atherosclerosis, we performed a decision curve analysis (Figure 4). The key aspect of the decision curve analysis is to investigate which diagnostic strategy leads the highest net benefit. The grey line corresponded to the net benefit for "treat all" strategy, i.e. performed 2D and/or 3D GLS in all patients who presented with chest pain. Conversely, the solid black line corresponded to the net benefit for "treat none" strategy, i.e. do not perform 2D and/or 3D GLS in any patients. The green dotted line reflected the model that included 2D GLS and it showed the greatest net benefit (i.e. overall "highest" line) across most threshold probabilities compared to 3D GLS. In other words, 2D GLS is the best predictor of presence of coronary atherosclerosis as compared to 3D GLS or age in this decision curve analysis.

Figure 4 Decision curve analysis using predictive models of two-dimensional global longitudinal strain, three-dimensional global longitudinal strain or age

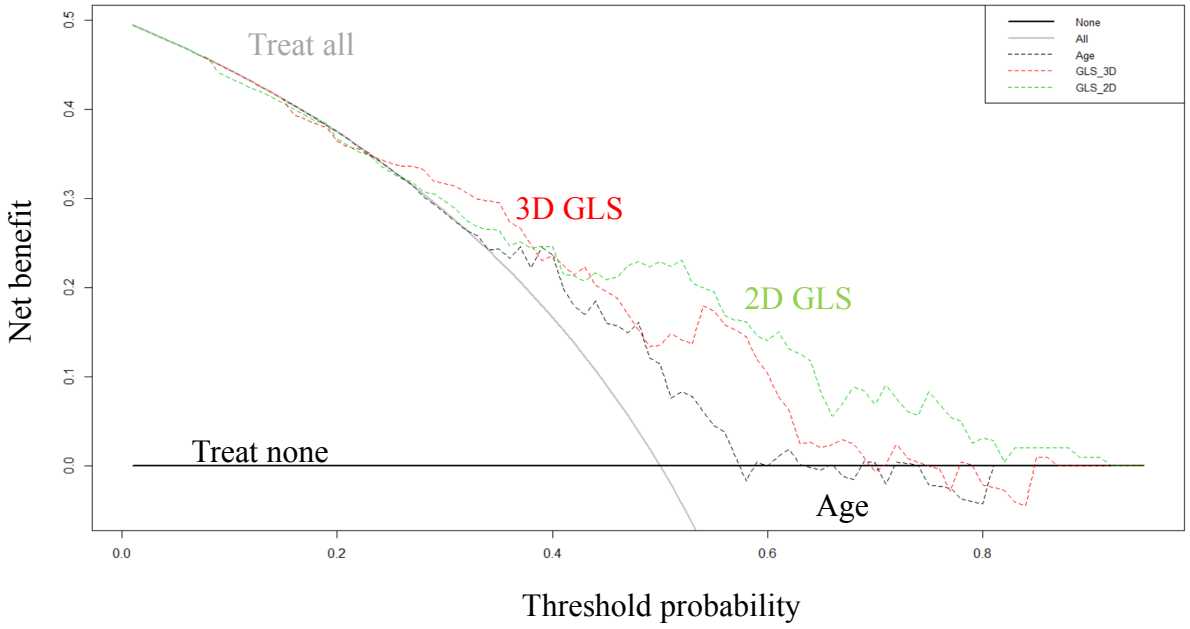

2D: 2-dimensional; 3D: 3-dimensional; GLS: global longitudinal strain.

4.4 Discussion

The present study sought to determine whether the presence of non-obstructive CAD has an impact on LV myocardial strain in patients with preserved LV EF as well as assess the predictive values of 2D versus 3D GLS in identifying subclinical CAD in the absence of traditional cardiac risk factors. The strength of our study is the exclusion of known confounders for impaired GLS such as hypertension, diabetes and obstructive CAD. We demonstrated that: 1) non-obstructive coronary atherosclerosis was associated with lower 2D and 3D GLS; and 2) 2D GLS was superior to 3D GLS in predicting the presence of coronary atherosclerosis in patients with low risk chest pain.

4.4.1 Causes of subclinical left ventricular dysfunction

The underlying pathophysiological process causing subclinical myocardial dysfunction in cardiac patients can be quite varied. Foremost, obstructive CAD resulting in myocardial ischaemia is well known for causing subclinical LV dysfunction despite preservation of conventional indices of systolic LV function and no overt infarction (154). As the severity of coronary stenosis increases and coronary flow becomes critically reduced in the subendocardium, the frequency of demand-induced ischaemia increases (154). Additionally, chronic repetitive ischaemia may cause chronic myocardial stunning and hibernation (190). However, in the setting of non-flow limiting coronary stenosis, this hypothesis is unlikely. Secondly, cardiac risk factors including hypertension and diabetes have been shown to be associated with subclinical myocardial dysfunction (151-154). These conditions are often associated with endothelial dysfunction leading to small vessel ischaemia, increased interstitial fibrosis and subsequent myocardial dysfunction.

Compared to previous studies, our study incrementally added to the scientific literature by demonstrating an association between subclinical LV dysfunction assessed by 2D and 3D GLS and non-obstructive CAD, independent of hypertension or diabetes. Though this association does not equate to causality, this finding suggests an alternative pathophysiological process that contribute to myocardial dysfunction independent of reduced coronary flow and other conventional cardiac risk factors such as hypertension or diabetes. We have previously demonstrated that patients with increased EAT volume is associated with subclinical LV dysfunction (191).

4.4.2 Two-dimensional versus three-dimensional speckle tracking echocardiography in assessing left ventricular function and detecting coronary atherosclerosis

2D STE is currently the most common method in quantifying LV myocardial deformation. However, LV myocardial through-plane and twisting motions are known to potentially affect the calculation of 2D strain values (126). 3D echocardiography and STE may overcome these limitations and allows the calculation of LV EF, volumentric analysis, and simultaneous measurement of multidirectional strains in a single volume dataset (146). Despite being technically more demanding to acquire 3D dataset, previous studies suggested that quantification of 3D GLS was less time intensive compared to 2D GLS (136, 137, 145).

However, 2D and 3D GLS are not interchangeable (137, 146-149). Previous studies have suggested that 3D GLS had a better correlation with LV EF compared to 2D GLS (144, 148, 173). Furthermore, 3D STE was shown to be more accurate and reproducible than 2D STE, especially for radial and circumferential evaluations (145).

2D GLS has been shown to predict the presence of significant CAD (158-167, 169, 192). Additionally, 2D GLS is inversely related to the number of stenotic coronary vessels (162, 163). On the other hand, the role of 3D STE in CAD is less well established with conflicting published results. Li and coworkers demonstrated the 3D multidirectional strain was predictive of moderate and severe CAD (AUC of 0.899 and 0.896 respectively) (174). Sun and co-workers found opposing results where 3D multi-directional peak strains were not diagnostic of CAD (defined as > 25% coronary stenosis) in patients with suspected angina (175). However, they found that a composite measurement of peak LS and time to peak LS was predictive of mild-severe CAD (AUC of 0.692) (175). To our best knowledge, this is the first study to compare 2D versus 3D STE for the detection of non-obstructive coronary atherosclerosis in patients with low risk chest pain. We sought to compare the sensitivity and clinical usefulness of 2D versus 3D GLS to detect the subtlest of differences in patients with

no CAD versus non-obstructive CAD, and without any potential confounders such as hypertension or diabetes. We demonstrated that both 2D and 3D GLS were lower in patients with non-obstructive CAD (receiver operating characteristic curve with area under the curve of 0.70, 0.65 respectively), but 3D GLS failed to demonstrate superiority over 2D GLS on decision curve analysis. Our findings are in contrary to previous studies which demonstrated the superiority of 3D over 2D STE in terms of LV function assessment (144, 145, 148, 173). This could partly be explained by the inherent technical difficulty of 3D STE as its temporal and spatial resolutions are lower compared to 2D STE (140). Even though lower frame rate in 3D STE has not been shown to affect accuracy of strain measurement by Yodwut and co-workers (142), the generalizability of their results may be limited due to small patient sample size of only 16 normal volunteers and 11 patients. In contrast, our experience suggested higher technical challenges in the acquisition and analysis of 3D speckle tracking in a much larger real-life clinical patient cohort. In addition, stitch artefacts may be unavoidable in uncooperative patients and in those with cardiac arrhythmias i.e. atrial fibrillation (140). However, in our study, all 3D images were obtained with breath holding to avoid stitch artefacts, and patients with cardiac arrhythmias were exclusion by the study design. Therefore, we would expect much lower 3D STE feasibility in routine clinical practice.

4.5 Conclusions

Non-obstructive CAD is an independent determinant of subclinical LV dysfunction. Despite the potential theoretical advantages of 3D STE, 2D STE is superior in predicting coronary atherosclerosis in patients with low risk chest pain without the presence of confounding co-morbidities such as hypertension and diabetes. Further larger studies are needed to assess the clinical applicability of early diagnosis and management of non-obstructive CAD.

CHAPTER FIVE

Conclusions of research project

GLS has been shown to be a useful echocardiographic parameter to refine risk stratification of patients with low risk chest pain. In our study, 2D STE seems to be superior to 3D STE in predicting coronary atherosclerosis in patients with no significant conventional cardiac risk factors such as hypertension and diabetes. Speckle tracking echocardiographic technique is relatively easy to use and is readily available in most echocardiography laboratories, and could be incorporated into daily routine clinical practice.

Both non-obstructive CAD and EAT are independent determinants of GLS in our studies. This added to the body of evidence in the current literature on EAT and coronary atherosclerosis and myocardial dysfunction. Though the association between EAT and coronary atherosclerosis has been widely reported, our studies suggested a separate pathological process independent of coronary ischaemia that leads to subclinical myocardial dysfunction. It has been proposed to be secondary to abnormal myocardial lipid and energy homeostasis, steatosis and lipotoxicity. EAT and non-flowing limiting coronary atherosclerosis may share these common pathophysiological pathways towards subclinical LV dysfunction.

In conclusion, we highlight the potential role of EAT and non-obstructive coronary atherosclerosis in the pathogenesis of subclinical myocardial dysfunction. Future studies are needed to further validate these determinants of myocardial deformation and the clinical applicability and benefit of identifying and managing these non-conventional cardiac “risk factors” for patients with low risk chest pain.

REFERENCES

1. Fox CS, Massaro JM, Hoffmann U, Pou KM, Maurovich-Horvat P, Liu CY, et al. Abdominal visceral and subcutaneous adipose tissue compartments: association with metabolic risk factors in the Framingham Heart Study. Circulation. 2007;116(1):39-48.

2. Iacobellis G, Assael F, Ribaudo MC, Zappaterreno A, Alessi G, Di Mario U, et al. Epicardial fat from echocardiography: a new method for visceral adipose tissue prediction. Obesity research. 2003;11(2):304-10.

3. Kahn HS, Austin H, Williamson DF, Arensberg D. Simple anthropometric indices associated with ischemic heart disease. Journal of clinical epidemiology. 1996;49(9):1017-24.

4. DeFronzo RA. Insulin resistance, lipotoxicity, type 2 diabetes and atherosclerosis: the missing links. The Claude Bernard Lecture 2009. Diabetologia. 2010;53(7):1270-87.

5. Gastaldelli A, Basta G. Ectopic fat and cardiovascular disease: what is the link? Nutrition, metabolism, and cardiovascular diseases : NMCD. 2010;20(7):481-90.

6. Cetin Mea. Effect of epicardial adipose tissue on diastolic functions and left atrial dimension in untreated hypertensive patients with normal systolic function. Journal of Cardiology. 2013;61:369-4.

7. Malavazos AE, Di Leo G, Secchi F, Lupo EN, Dogliotti G, Coman C, et al. Relation of echocardiographic epicardial fat thickness and myocardial fat. The American journal of cardiology. 2010;105(12):1831-5.

8. Gaborit B, Abdesselam I, Dutour A. Epicardial fat: more than just an "epi" phenomenon? Hormone and metabolic research = Hormon- und Stoffwechselforschung = Hormones et metabolisme. 2013;45(13):991-1001.

9. Kilicaslan B, Ozdogan O, Aydin M, Dursun H, Susam I, Ertas F. Increased epicardial fat thickness is associated with cardiac functional changes in healthy women. The Tohoku journal of experimental medicine. 2012;228(2):119-24.

10. Iacobellis G, Pistilli D, Gucciardo M, Leonetti F, Miraldi F, Brancaccio G, et al. Adiponectin expression in human epicardial adipose tissue in vivo is lower in patients with coronary artery disease. Cytokine. 2005;29(6):251-5.

11. Iacobellis G, Willens HJ. Echocardiographic epicardial fat: a review of research and clinical applications. Journal of the American Society of Echocardiography : official publication of the American Society of Echocardiography. 2009;22(12):1311-9; quiz 417-8.

12. Silaghi AC, Poanta L, Valea A, Pais R, Silaghi H. Is epicardial adipose tissue, assessed by echocardiography, a reliable method for visceral adipose tissue prediction? Medical ultrasonography. 2011;13(1):15-20.

13. Tok D, Cagli K, Kadife I, Turak O, Ozcan F, Basar FN, et al. Impaired coronary flow reserve is associated with increased echocardiographic epicardial fat thickness in metabolic syndrome patients. Coronary artery disease. 2013;24(3):191-5.

14. Corradi D, Maestri R, Callegari S, Pastori P, Goldoni M, Luong TV, et al. The ventricular epicardial fat is related to the myocardial mass in normal, ischemic and hypertrophic hearts. Cardiovascular pathology : the official journal of the Society for Cardiovascular Pathology. 2004;13(6):313-6.

15. Sacks HS, Fain JN. Human epicardial adipose tissue: a review. Am Heart J. 2007;153(6):907-17.

16. McLean DS. Epicardial adipose tissue as a cardiovascular risk marker. Clin Lipidol. 2009;4:55-62.

17. Talman AH, Psaltis PJ, Cameron JD, Meredith IT, Seneviratne SK, Wong DT. Epicardial adipose tissue: far more than a fat depot. Cardiovascular diagnosis and therapy. 2014;4(6):416-29.

18. Morelli M, Gaggini M, Daniele G, Marraccini P, Sicari R, Gastaldelli A. Ectopic fat: the true culprit linking obesity and cardiovascular disease? Thrombosis and haemostasis. 2013;110(4):651-60.

19. Iacobellis G, Bianco AC. Epicardial adipose tissue: emerging physiological, pathophysiological and clinical features. Trends in endocrinology and metabolism: TEM. 2011;22(11):450-7.

20. Marchington JM, Mattacks CA, Pond CM. Adipose tissue in the mammalian heart and pericardium: structure, foetal development and biochemical properties. Comparative biochemistry and physiology B, Comparative biochemistry. 1989;94(2):225-32.

21. Marchington JM, Pond CM. Site-specific properties of pericardial and epicardial adipose tissue: the effects of insulin and high-fat feeding on lipogenesis and the incorporation of fatty acids in vitro. International journal of obesity. 1990;14(12):1013-22.

22. Rabkin SW. Epicardial fat: properties, function and relationship to obesity. Obesity reviews : an official journal of the International Association for the Study of Obesity. 2007;8(3):253-61.

23. Kaplan S, Ozturk M, Kiris G, Kaplan ST. Evaluation of therelationship between epicardial adipose tissue and myocardial performance (Tei) index. International journal of clinical and experimental medicine. 2014;7(6):1598-602.

24. Wende AR, Symons JD, Abel ED. Mechanisms of lipotoxicity in the cardiovascular system. Current hypertension reports. 2012;14(6):517-31.

25. Iacobellis G, di Gioia CR, Di Vito M, Petramala L, Cotesta D, De Santis V, et al. Epicardial adipose tissue and intracoronary adrenomedullin levels in coronary artery disease. Hormone and metabolic research = Hormon- und Stoffwechselforschung = Hormones et metabolisme. 2009;41(12):855-60.

26. Iacobellis G, di Gioia CR, Cotesta D, Petramala L, Travaglini C, De Santis V, et al. Epicardial adipose tissue adiponectin expression is related to intracoronary adiponectin levels. Hormone and metabolic research = Hormon- und Stoffwechselforschung = Hormones et metabolisme. 2009;41(3):227-31.

27. Kremen J, Dolinkova M, Krajickova J, Blaha J, Anderlova K, Lacinova Z, et al. Increased subcutaneous and epicardial adipose tissue production of proinflammatory cytokines in cardiac surgery patients: possible role in postoperative insulin resistance. The Journal of clinical endocrinology and metabolism. 2006;91(11):4620-7.

28. Cheng KH, Chu CS, Lee KT, Lin TH, Hsieh CC, Chiu CC, et al. Adipocytokines and proinflammatory mediators from abdominal and epicardial adipose tissue in patients with coronary artery disease. Int J Obes (Lond). 2008;32(2):268-74.

29. Fain JN, Sacks HS, Buehrer B, Bahouth SW, Garrett E, Wolf RY, et al. Identification of omentin mRNA in human epicardial adipose tissue: comparison to omentin in subcutaneous, internal mammary artery periadventitial and visceral abdominal depots. Int J Obes (Lond). 2008;32(5):810-5.

30. Moreno PR, Purushothaman KR, Fuster V, O'Connor WN. Intimomedial interface damage and adventitial inflammation is increased beneath disrupted atherosclerosis in the aorta: implications for plaque vulnerability. Circulation. 2002;105(21):2504-11.

31. Sharma AM. Adipose tissue: a mediator of cardiovascular risk. International journal of obesity and related metabolic disorders : journal of the International Association for the Study of Obesity. 2002;26 Suppl 4:S5-7.

32. Libby P, Ridker PM, Maseri A. Inflammation and atherosclerosis. Circulation. 2002;105(9):1135-43.

33. Gorter PM, van Lindert AS, de Vos AM, Meijs MF, van der Graaf Y, Doevendans PA, et al. Quantification of epicardial and peri-coronary fat using cardiac computed

tomography; reproducibility and relation with obesity and metabolic syndrome in patients suspected of coronary artery disease. Atherosclerosis. 2008;197(2):896-903.

34. Shimokawa H, Ito A, Fukumoto Y, Kadokami T, Nakaike R, Sakata M, et al. Chronic treatment with interleukin-1 beta induces coronary intimal lesions and vasospastic responses in pigs in vivo. The role of platelet-derived growth factor. The Journal of clinical investigation. 1996;97(3):769-76.

35. Miyata K, Shimokawa H, Kandabashi T, Higo T, Morishige K, Eto Y, et al. Rho-kinase is involved in macrophage-mediated formation of coronary vascular lesions in pigs in vivo. Arteriosclerosis, thrombosis, and vascular biology. 2000;20(11):2351-8.

36. Mazurek T, Zhang L, Zalewski A, Mannion JD, Diehl JT, Arafat H, et al. Human epicardial adipose tissue is a source of inflammatory mediators. Circulation. 2003;108(20):2460-6.

37. Eiras S, Teijeira-Fernandez E, Shamagian LG, Fernandez AL, Vazquez-Boquete A, Gonzalez-Juanatey JR. Extension of coronary artery disease is associated with increased IL-6 and decreased adiponectin gene expression in epicardial adipose tissue. Cytokine. 2008;43(2):174-80.

38. Baker AR, Silva NF, Quinn DW, Harte AL, Pagano D, Bonser RS, et al. Human epicardial adipose tissue expresses a pathogenic profile of adipocytokines in patients with cardiovascular disease. Cardiovascular diabetology. 2006;5:1.

39. Hirata Y, Tabata M, Kurobe H, Motoki T, Akaike M, Nishio C, et al. Coronary atherosclerosis is associated with macrophage polarization in epicardial adipose tissue. Journal of the American College of Cardiology. 2011;58(3):248-55.

40. Mahabadi AA, Reinsch N, Lehmann N, Altenbernd J, Kalsch H, Seibel RM, et al. Association of pericoronary fat volume with atherosclerotic plaque burden in the underlying coronary artery: a segment analysis. Atherosclerosis. 2010;211(1):195-9.

41. Laine P, Kaartinen M, Penttila A, Panula P, Paavonen T, Kovanen PT. Association between myocardial infarction and the mast cells in the adventitia of the infarct-related coronary artery. Circulation. 1999;99(3):361-9.

42. Konishi M, Sugiyama S, Sato Y, Oshima S, Sugamura K, Nozaki T, et al. Pericardial fat inflammation correlates with coronary artery disease. Atherosclerosis. 2010;213(2):649-55.

43. Barandier C, Montani JP, Yang Z. Mature adipocytes and perivascular adipose tissue stimulate vascular smooth muscle cell proliferation: effects of aging and obesity. American journal of physiology Heart and circulatory physiology. 2005;289(5):H1807-13.

44. Soltis EE, Cassis LA. Influence of perivascular adipose tissue on rat aortic smooth muscle responsiveness. Clinical and experimental hypertension Part A, Theory and practice. 1991;13(2):277-96.

45. Dubrovska G, Verlohren S, Luft FC, Gollasch M. Mechanisms of ADRF release from rat aortic adventitial adipose tissue. American journal of physiology Heart and circulatory physiology. 2004;286(3):H1107-13.

46. Lohn M, Dubrovska G, Lauterbach B, Luft FC, Gollasch M, Sharma AM. Periadventitial fat releases a vascular relaxing factor. FASEB journal : official publication of the Federation of American Societies for Experimental Biology. 2002;16(9):1057-63.

47. Iacobellis G, Malavazos AE, Corsi MM. Epicardial fat: from the biomolecular aspects to the clinical practice. The international journal of biochemistry & cell biology. 2011;43(12):1651-4.

48. Prati F, Arbustini E, Labellarte A, Sommariva L, Pawlowski T, Manzoli A, et al. Eccentric atherosclerotic plaques with positive remodelling have a pericardial distribution: a permissive role of epicardial fat? A three-dimensional intravascular ultrasound study of left anterior descending artery lesions. European heart journal. 2003;24(4):329-36.

49. Ahn SG, Lim HS, Joe DY, Kang SJ, Choi BJ, Choi SY, et al. Relationship of epicardial adipose tissue by echocardiography to coronary artery disease. Heart. 2008;94(3):e7.

50. Jeong JW, Jeong MH, Yun KH, Oh SK, Park EM, Kim YK, et al. Echocardiographic epicardial fat thickness and coronary artery disease. Circulation journal : official journal of the Japanese Circulation Society. 2007;71(4):536-9.

51. Eroglu S, Sade LE, Yildirir A, Bal U, Ozbicer S, Ozgul AS, et al. Epicardial adipose tissue thickness by echocardiography is a marker for the presence and severity of coronary artery disease. Nutrition, metabolism, and cardiovascular diseases : NMCD. 2009;19(3):211-7.

52. Shemirani H, Khoshavi M. Correlation of echocardiographic epicardial fat thickness with severity of coronary artery disease-an observational study. Anadolu kardiyoloji dergisi : AKD = the Anatolian journal of cardiology. 2012;12(3):200-5.

53. Sarin S, Wenger C, Marwaha A, Qureshi A, Go BD, Woomert CA, et al. Clinical significance of epicardial fat measured using cardiac multislice computed tomography. The American journal of cardiology. 2008;102(6):767-71.

54. Djaberi R, Schuijf JD, van Werkhoven JM, Nucifora G, Jukema JW, Bax JJ. Relation of epicardial adipose tissue to coronary atherosclerosis. The American journal of cardiology. 2008;102(12):1602-7.

55. Bastarrika G, Broncano J, Schoepf UJ, Schwarz F, Lee YS, Abro JA, et al. Relationship between coronary artery disease and epicardial adipose tissue quantification at cardiac CT: comparison between automatic volumetric measurement and manual bidimensional estimation. Academic radiology. 2010;17(6):727-34.

56. Iwasaki K, Matsumoto T, Aono H, Furukawa H, Samukawa M. Relationship between epicardial fat measured by 64-multidetector computed tomography and coronary artery disease. Clinical cardiology. 2011;34(3):166-71.

57. Oka T, Yamamoto H, Ohashi N, Kitagawa T, Kunita E, Utsunomiya H, et al. Association between epicardial adipose tissue volume and characteristics of non-calcified plaques assessed by coronary computed tomographic angiography. International journal of cardiology. 2012;161(1):45-9.

58. Alexopoulos N, McLean DS, Janik M, Arepalli CD, Stillman AE, Raggi P. Epicardial adipose tissue and coronary artery plaque characteristics. Atherosclerosis. 2010;210(1):150-4.

59. Greif M, Becker A, von Ziegler F, Lebherz C, Lehrke M, Broedl UC, et al. Pericardial adipose tissue determined by dual source CT is a risk factor for coronary atherosclerosis. Arteriosclerosis, thrombosis, and vascular biology. 2009;29(5):781-6.

60. Ueno K, Anzai T, Jinzaki M, Yamada M, Jo Y, Maekawa Y, et al. Increased epicardial fat volume quantified by 64-multidetector computed tomography is associated with coronary atherosclerosis and totally occlusive lesions. Circulation journal : official journal of the Japanese Circulation Society. 2009;73(10):1927-33.

61. Bettencourt N, Toschke AM, Leite D, Rocha J, Carvalho M, Sampaio F, et al. Epicardial adipose tissue is an independent predictor of coronary atherosclerotic burden. International journal of cardiology. 2012;158(1):26-32.

62. Janik M, Hartlage G, Alexopoulos N, Mirzoyev Z, McLean DS, Arepalli CD, et al. Epicardial adipose tissue volume and coronary artery calcium to predict myocardial ischemia on positron emission tomography-computed tomography studies. Journal of nuclear cardiology : official publication of the American Society of Nuclear Cardiology. 2010;17(5):841-7.

63. Nakanishi R, Rajani R, Cheng VY, Gransar H, Nakazato R, Shmilovich H, et al. Increase in epicardial fat volume is associated with greater coronary artery calcification progression in subjects at intermediate risk by coronary calcium score: a serial study using non-contrast cardiac CT. Atherosclerosis. 2011;218(2):363-8.

64. Bachar GN, Dicker D, Kornowski R, Atar E. Epicardial adipose tissue as a predictor of coronary artery disease in asymptomatic subjects. The American journal of cardiology. 2012;110(4):534-8.

65. Tamarappoo B, Dey D, Shmilovich H, Nakazato R, Gransar H, Cheng VY, et al. Increased pericardial fat volume measured from noncontrast CT predicts myocardial ischemia by SPECT. JACC Cardiovascular imaging. 2010;3(11):1104-12.

66. de Vos AM, Prokop M, Roos CJ, Meijs MF, van der Schouw YT, Rutten A, et al. Peri-coronary epicardial adipose tissue is related to cardiovascular risk factors and coronary artery calcification in post-menopausal women. European heart journal. 2008;29(6):777-83.

67. Ding J, Kritchevsky SB, Harris TB, Burke GL, Detrano RC, Szklo M, et al. The association of pericardial fat with calcified coronary plaque. Obesity. 2008;16(8):1914-9.

68. Rosito GA, Massaro JM, Hoffmann U, Ruberg FL, Mahabadi AA, Vasan RS, et al. Pericardial fat, visceral abdominal fat, cardiovascular disease risk factors, and vascular calcification in a community-based sample: the Framingham Heart Study. Circulation. 2008;117(5):605-13.

69. Ding J, Hsu FC, Harris TB, Liu Y, Kritchevsky SB, Szklo M, et al. The association of pericardial fat with incident coronary heart disease: the Multi-Ethnic Study of Atherosclerosis (MESA). The American journal of clinical nutrition. 2009;90(3):499-504.

70. Sade LE, Eroglu S, Bozbas H, Ozbicer S, Hayran M, Haberal A, et al. Relation between epicardial fat thickness and coronary flow reserve in women with chest pain and angiographically normal coronary arteries. Atherosclerosis. 2009;204(2):580-5.

71. Comert N, Yucel O, Ege MR, Yaylak B, Erdogan G, Yilmaz MB. Echocardiographic epicardial adipose tissue predicts subclinical atherosclerosis: epicardial adipose tissue and atherosclerosis. Angiology. 2012;63(8):586-90.

72. Alam MS, Green R, de Kemp R, Beanlands RS, Chow BJ. Epicardial adipose tissue thickness as a predictor of impaired microvascular function in patients with non-obstructive coronary artery disease. Journal of nuclear cardiology : official publication of the American Society of Nuclear Cardiology. 2013;20(5):804-12.

73. Chaowalit N, Somers VK, Pellikka PA, Rihal CS, Lopez-Jimenez F. Subepicardial adipose tissue and the presence and severity of coronary artery disease. Atherosclerosis. 2006;186(2):354-9.

74. Gorter PM, de Vos AM, van der Graaf Y, Stella PR, Doevendans PA, Meijs MF, et al. Relation of epicardial and pericoronary fat to coronary atherosclerosis and coronary artery calcium in patients undergoing coronary angiography. The American journal of cardiology. 2008;102(4):380-5.

75. Vural M, Talu A, Sahin D, Elalmis OU, Durmaz HA, Uyanik S, et al. Evaluation of the relationship between epicardial fat volume and left ventricular diastolic dysfunction. Japanese journal of radiology. 2014;32(6):331-9.

76. Morricone L, Malavazos AE, Coman C, Donati C, Hassan T, Caviezel F. Echocardiographic abnormalities in normotensive obese patients: relationship with visceral fat. Obesity research. 2002;10(6):489-98.

77. Nakajima T, Fujioka S, Tokunaga K, Matsuzawa Y, Tarui S. Correlation of intraabdominal fat accumulation and left ventricular performance in obesity. The American journal of cardiology. 1989;64(5):369-73.

78. Humphries MC, Gutin B, Barbeau P, Vemulapalli S, Allison J, Owens S. Relations of adiposity and effects of training on the left ventricle in obese youths. Medicine and science in sports and exercise. 2002;34(9):1428-35.

79. Vetta F, Cicconetti P, Ronzoni S, Rizzo V, Palleschi L, Canarile G, et al. Hyperinsulinaemia, regional adipose tissue distribution and left ventricular mass in normotensive, elderly, obese subjects. European heart journal. 1998;19(2):326-31.

80. Iacobellis G, Ribaudo MC, Zappaterreno A, Iannucci CV, Leonetti F. Relation between epicardial adipose tissue and left ventricular mass. The American journal of cardiology. 2004;94(8):1084-7.

81. Mookadam F, Goel R, Alharthi MS, Jiamsripong P, Cha S. Epicardial fat and its association with cardiovascular risk: a cross-sectional observational study. Heart views : the official journal of the Gulf Heart Association. 2010;11(3):103-8.

82. Fox CS, Gona P, Hoffmann U, Porter SA, Salton CJ, Massaro JM, et al. Pericardial fat, intrathoracic fat, and measures of left ventricular structure and function: the Framingham Heart Study. Circulation. 2009;119(12):1586-91.

83. Nyman K, Graner M, Pentikainen MO, Lundbom J, Hakkarainen A, Siren R, et al. Cardiac steatosis and left ventricular function in men with metabolic syndrome. J Cardiovasc Magn Reson. 2013;15:103.

84. Iacobellis G, Leonetti F, Singh N, A MS. Relationship of epicardial adipose tissue with atrial dimensions and diastolic function in morbidly obese subjects. International journal of cardiology. 2007;115(2):272-3.

85. Venteclef N, Guglielmi V, Balse E, Gaborit B, Cotillard A, Atassi F, et al. Human epicardial adipose tissue induces fibrosis of the atrial myocardium through the secretion of adipo-fibrokines. European heart journal. 2013.

86. Schaffer JE. Lipotoxicity: when tissues overeat. Current opinion in lipidology. 2003;14(3):281-7.

87. Liu CY, Bluemke DA, Gerstenblith G, Zimmerman SL, Li J, Zhu H, et al. Myocardial steatosis and its association with obesity and regional ventricular dysfunction: evaluated by magnetic resonance tagging and 1H spectroscopy in healthy African Americans. International journal of cardiology. 2014;172(2):381-7.

88. Chiu HC, Kovacs A, Ford DA, Hsu FF, Garcia R, Herrero P, et al. A novel mouse model of lipotoxic cardiomyopathy. The Journal of clinical investigation. 2001;107(7):813-22.

89. Zhou YT, Grayburn P, Karim A, Shimabukuro M, Higa M, Baetens D, et al. Lipotoxic heart disease in obese rats: implications for human obesity. Proceedings of the National Academy of Sciences of the United States of America. 2000;97(4):1784-9.

90. Szczepaniak LS, Dobbins RL, Metzger GJ, Sartoni-D'Ambrosia G, Arbique D, Vongpatanasin W, et al. Myocardial triglycerides and systolic function in humans: in vivo evaluation by localized proton spectroscopy and cardiac imaging. Magnetic resonance in medicine : official journal of the Society of Magnetic Resonance in Medicine / Society of Magnetic Resonance in Medicine. 2003;49(3):417-23.

91. Sharma S, Adrogue JV, Golfman L, Uray I, Lemm J, Youker K, et al. Intramyocardial lipid accumulation in the failing human heart resembles the lipotoxic rat heart. FASEB journal : official publication of the Federation of American Societies for Experimental Biology. 2004;18(14):1692-700.

92. Glenn DJ, Wang F, Nishimoto M, Cruz MC, Uchida Y, Holleran WM, et al. A murine model of isolated cardiac steatosis leads to cardiomyopathy. Hypertension. 2011;57(2):216-22.

93. Christoffersen C, Bollano E, Lindegaard ML, Bartels ED, Goetze JP, Andersen CB, et al. Cardiac lipid accumulation associated with diastolic dysfunction in obese mice. Endocrinology. 2003;144(8):3483-90.

94. McGavock JM, Victor RG, Unger RH, Szczepaniak LS, American College of P, the American Physiological S. Adiposity of the heart, revisited. Annals of internal medicine. 2006;144(7):517-24.

95. Ng AC, Delgado V, Djaberi R, Schuijf JD, Boogers MJ, Auger D, et al. Multimodality imaging in diabetic heart disease. Curr Probl Cardiol. 2011;36(1):9-47.

96. Liu J, Fox CS, Hickson DA, May WL, Ding J, Carr JJ, et al. Pericardial fat and echocardiographic measures of cardiac abnormalities: the Jackson Heart Study. Diabetes care. 2011;34(2):341-6.

97. Iacobellis A, Marcellini M, Andriulli A, Perri F, Leandro G, Devito R, et al. Non invasive evaluation of liver fibrosis in paediatric patients with nonalcoholic steatohepatitis. World journal of gastroenterology : WJG. 2006;12(48):7821-5.

98. Cavalcante JL, Tamarappoo BK, Hachamovitch R, Kwon DH, Alraies MC, Halliburton S, et al. Association of epicardial fat, hypertension, subclinical coronary artery disease, and metabolic syndrome with left ventricular diastolic dysfunction. The American journal of cardiology. 2012;110(12):1793-8.

99. Marwan M, Achenbach S. Quantification of epicardial fat by computed tomography: why, when and how? J Cardiovasc Comput Tomogr. 2013;7(1):3-10.

100. Sironi AM, Pingitore A, Ghione S, De Marchi D, Scattini B, Positano V, et al. Early hypertension is associated with reduced regional cardiac function, insulin resistance, epicardial, and visceral fat. Hypertension. 2008;51(2):282-8.

101. Erdogan T, Cetin M, Kocaman SA, Durakoglugil ME, Ergul E, Ugurlu Y, et al. Epicardial adipose tissue is independently associated with increased left ventricular mass in

untreated hypertensive patients: an observational study. Anadolu kardiyoloji dergisi : AKD = the Anatolian journal of cardiology. 2013;13(4):320-7.

102. Turak O, Ozcan F, Canpolat U, Isleyen A, Cebeci M, Oksuz F, et al. Increased echocardiographic epicardial fat thickness and high-sensitivity CRP level indicate diastolic dysfunction in patients with newly diagnosed essential hypertension. Blood pressure monitoring. 2013;18(5):259-64.

103. Dabbah S, Komarov H, Marmor A, Assy N. Epicardial fat, rather than pericardial fat, is independently associated with diastolic filling in subjects without apparent heart disease. Nutrition, metabolism, and cardiovascular diseases : NMCD. 2014;24(8):877-82.

104. Konishi M, Sugiyama S, Sugamura K, Nozaki T, Matsubara J, Akiyama E, et al. Accumulation of pericardial fat correlates with left ventricular diastolic dysfunction in patients with normal ejection fraction. J Cardiol. 2012;59(3):344-51.

105. Hachiya K, Fukuta H, Wakami K, Goto T, Tani T, Ohte N. Relation of epicardial fat to central aortic pressure and left ventricular diastolic function in patients with known or suspected coronary artery disease. The international journal of cardiovascular imaging. 2014;30(7):1393-8.

106. Park HE, Choi SY, Kim M. Association of epicardial fat with left ventricular diastolic function in subjects with metabolic syndrome: assessment using 2-dimensional echocardiography. BMC cardiovascular disorders. 2014;14:3.

107. Fluchter S, Haghi D, Dinter D, Heberlein W, Kuhl HP, Neff W, et al. Volumetric assessment of epicardial adipose tissue with cardiovascular magnetic resonance imaging. Obesity. 2007;15(4):870-8.

108. Doesch C, Haghi D, Fluchter S, Suselbeck T, Schoenberg SO, Michaely H, et al. Epicardial adipose tissue in patients with heart failure. J Cardiovasc Magn Reson. 2010;12:40.

109. Doesch C, Suselbeck T, Haghi D, Streitner F, Schoenberg SO, Borggrefe M, et al. The relationship between the severity of coronary artery disease and epicardial adipose tissue depends on the left ventricular function. PloS one. 2012;7(11):e48330.

110. Khawaja T, Greer C, Chokshi A, Chavarria N, Thadani S, Jones M, et al. Epicardial fat volume in patients with left ventricular systolic dysfunction. The American journal of cardiology. 2011;108(3):397-401.

111. Doesch C, Streitner F, Bellm S, Suselbeck T, Haghi D, Heggemann F, et al. Epicardial adipose tissue assessed by cardiac magnetic resonance imaging in patients with heart failure due to dilated cardiomyopathy. Obesity. 2013;21(3):E253-61.

112. Tabakci MM, Durmus HI, Avci A, Toprak C, Demir S, Arslantas U, et al. Relation of Epicardial Fat Thickness to the Severity of Heart Failure in Patients with Nonischemic Dilated Cardiomyopathy. Echocardiography. 2014.

113. Iacobellis G, Zaki MC, Garcia D, Willens HJ. Epicardial fat in atrial fibrillation and heart failure. Hormone and metabolic research = Hormon- und Stoffwechselforschung = Hormones et metabolisme. 2014;46(8):587-90.

114. Karayannis G, Giamouzis G, Tziolas N, Georgoulias P, Skoularigis J, Mikhailidis DP, et al. Association between epicardial fat thickness and weight homeostasis hormones in patients with noncachectic heart failure. Angiology. 2013;64(3):173-80.

115. Saura D, Oliva MJ, Rodriguez D, Pascual-Figal DA, Hurtado JA, Pinar E, et al. Reproducibility of echocardiographic measurements of epicardial fat thickness. International journal of cardiology. 2010;141(3):311-3.

116. Abbara S, Desai JC, Cury RC, Butler J, Nieman K, Reddy V. Mapping epicardial fat with multi-detector computed tomography to facilitate percutaneous transepicardial arrhythmia ablation. European journal of radiology. 2006;57(3):417-22.

117. Dey D, Wong ND, Tamarappoo B, Nakazato R, Gransar H, Cheng VY, et al. Computer-aided non-contrast CT-based quantification of pericardial and thoracic fat and their associations with coronary calcium and Metabolic Syndrome. Atherosclerosis. 2010;209(1):136-41.

118. Kankaanpaa M, Lehto HR, Parkka JP, Komu M, Viljanen A, Ferrannini E, et al. Myocardial triglyceride content and epicardial fat mass in human obesity: relationship to left ventricular function and serum free fatty acid levels. The Journal of clinical endocrinology and metabolism. 2006;91(11):4689-95.

119. Virtanen KA, Hallsten K, Parkkola R, Janatuinen T, Lonnqvist F, Viljanen T, et al. Differential effects of rosiglitazone and metformin on adipose tissue distribution and glucose uptake in type 2 diabetic subjects. Diabetes. 2003;52(2):283-90.

120. American College of Cardiology Foundation Task Force on Expert Consensus D, Hundley WG, Bluemke DA, Finn JP, Flamm SD, Fogel MA, et al. ACCF/ACR/AHA/NASCI/SCMR 2010 expert consensus document on cardiovascular magnetic resonance: a report of the American College of Cardiology Foundation Task Force on Expert Consensus Documents. Journal of the American College of Cardiology. 2010;55(23):2614-62.

121. Seo Y, Ishizu T, Atsumi A, Kawamura R, Aonuma K. Three-dimensional speckle tracking echocardiography. Circulation journal : official journal of the Japanese Circulation Society. 2014;78(6):1290-301.

122. Solomon SD, Anavekar N, Skali H, McMurray JJ, Swedberg K, Yusuf S, et al. Influence of ejection fraction on cardiovascular outcomes in a broad spectrum of heart failure patients. Circulation. 2005;112(24):3738-44.

123. Shah AM, Solomon SD. Myocardial deformation imaging: current status and future directions. Circulation. 2012;125(2):e244-8.

124. Marwick TH. The Clinical Application of Strain: Raising the Standard. Journal of the American Society of Echocardiography : official publication of the American Society of Echocardiography. 2015;28(10):1182-3.

125. Nasseri BA, Kukucka M, Dandel M, Knosalla C, Choi YH, Ebell W, et al. Two-dimensional speckle tracking strain analysis for efficacy assessment of myocardial cell therapy. Cell Transplant. 2009;18(3):361-70.

126. Wu VC, Takeuchi M, Otani K, Haruki N, Yoshitani H, Tamura M, et al. Effect of through-plane and twisting motion on left ventricular strain calculation: direct comparison between two-dimensional and three-dimensional speckle-tracking echocardiography. Journal of the American Society of Echocardiography : official publication of the American Society of Echocardiography. 2013;26(11):1274-81 e4.

127. Mondillo S, Galderisi M, Mele D, Cameli M, Lomoriello VS, Zaca V, et al. Speckle-tracking echocardiography: a new technique for assessing myocardial function. Journal of ultrasound in medicine : official journal of the American Institute of Ultrasound in Medicine. 2011;30(1):71-83.

128. Amundsen BH, Helle-Valle T, Edvardsen T, Torp H, Crosby J, Lyseggen E, et al. Noninvasive myocardial strain measurement by speckle tracking echocardiography: validation against sonomicrometry and tagged magnetic resonance imaging. Journal of the American College of Cardiology. 2006;47(4):789-93.

129. Collier P, Phelan D, Klein A. A Test in Context: Myocardial Strain Measured by Speckle-Tracking Echocardiography. Journal of the American College of Cardiology. 2017;69(8):1043-56.

130. Kleijn SA, Pandian NG, Thomas JD, Perez de Isla L, Kamp O, Zuber M, et al. Normal reference values of left ventricular strain using three-dimensional speckle tracking

echocardiography: results from a multicentre study. European heart journal cardiovascular Imaging. 2015;16(4):410-6.

131. Farsalinos KE, Daraban AM, Unlu S, Thomas JD, Badano LP, Voigt JU. Head-to-Head Comparison of Global Longitudinal Strain Measurements among Nine Different Vendors: The EACVI/ASE Inter-Vendor Comparison Study. Journal of the American Society of Echocardiography : official publication of the American Society of Echocardiography. 2015;28(10):1171-81, e2.

132. Wen H, Liang Z, Zhao Y, Yang K. Feasibility of detecting early left ventricular systolic dysfunction using global area strain: a novel index derived from three-dimensional speckle-tracking echocardiography. European journal of echocardiography : the journal of the Working Group on Echocardiography of the European Society of Cardiology. 2011;12(12):910-6.

133. Opdahl A, Helle-Valle T, Skulstad H, Smiseth OA. Strain, strain rate, torsion, and twist: echocardiographic evaluation. Current cardiology reports. 2015;17(3):568.

134. Altman M, Bergerot C, Aussoleil A, Davidsen ES, Sibellas F, Ovize M, et al. Assessment of left ventricular systolic function by deformation imaging derived from speckle tracking: a comparison between 2D and 3D echo modalities. European heart journal cardiovascular Imaging. 2014;15(3):316-23.

135. Biswas S, Ananthasubramaniam K. Clinical utility of three-dimensional echocardiography for the evaluation of ventricular function. Cardiology in review. 2013;21(4):184-95.

136. Perez de Isla L, Balcones DV, Fernandez-Golfin C, Marcos-Alberca P, Almeria C, Rodrigo JL, et al. Three-dimensional-wall motion tracking: a new and faster tool for myocardial strain assessment: comparison with two-dimensional-wall motion tracking.

Journal of the American Society of Echocardiography : official publication of the American Society of Echocardiography. 2009;22(4):325-30.

137. Saito K, Okura H, Watanabe N, Hayashida A, Obase K, Imai K, et al. Comprehensive evaluation of left ventricular strain using speckle tracking echocardiography in normal adults: comparison of three-dimensional and two-dimensional approaches. Journal of the American Society of Echocardiography : official publication of the American Society of Echocardiography. 2009;22(9):1025-30.

138. Duan F, Xie M, Wang X, Li Y, He L, Jiang L, et al. Preliminary clinical study of left ventricular myocardial strain in patients with non-ischemic dilated cardiomyopathy by three-dimensional speckle tracking imaging. Cardiovascular ultrasound. 2012;10:8.

139. Luis SA, Yamada A, Khandheria BK, Speranza V, Benjamin A, Ischenko M, et al. Use of three-dimensional speckle-tracking echocardiography for quantitative assessment of global left ventricular function: a comparative study to three-dimensional echocardiography. Journal of the American Society of Echocardiography : official publication of the American Society of Echocardiography. 2014;27(3):285-91.

140. Nesser HJ, Mor-Avi V, Gorissen W, Weinert L, Steringer-Mascherbauer R, Niel J, et al. Quantification of left ventricular volumes using three-dimensional echocardiographic speckle tracking: comparison with MRI. European heart journal. 2009;30(13):1565-73.

141. Cheung YF. The role of 3D wall motion tracking in heart failure. Nature reviews Cardiology. 2012;9(11):644-57.

142. Yodwut C, Weinert L, Klas B, Lang RM, Mor-Avi V. Effects of frame rate on three-dimensional speckle-tracking-based measurements of myocardial deformation. Journal of the American Society of Echocardiography : official publication of the American Society of Echocardiography. 2012;25(9):978-85.

143. Gayat E, Ahmad H, Weinert L, Lang RM, Mor-Avi V. Reproducibility and inter-vendor variability of left ventricular deformation measurements by three-dimensional speckle-tracking echocardiography. Journal of the American Society of Echocardiography : official publication of the American Society of Echocardiography. 2011;24(8):878-85.

144. Hayat D, Kloeckner M, Nahum J, Ecochard-Dugelay E, Dubois-Rande JL, Jean-Francois D, et al. Comparison of real-time three-dimensional speckle tracking to magnetic resonance imaging in patients with coronary heart disease. The American journal of cardiology. 2012;109(2):180-6.

145. Reant P, Barbot L, Touche C, Dijos M, Arsac F, Pillois X, et al. Evaluation of global left ventricular systolic function using three-dimensional echocardiography speckle-tracking strain parameters. Journal of the American Society of Echocardiography : official publication of the American Society of Echocardiography. 2012;25(1):68-79.

146. D'Ascenzi F, Solari M, Mazzolai M, Cameli M, Lisi M, Andrei V, et al. Two-dimensional and three-dimensional left ventricular deformation analysis: a study in competitive athletes. The international journal of cardiovascular imaging. 2016;32(12):1697-705.

147. Negishi K, Negishi T, Agler DA, Plana JC, Marwick TH. Role of temporal resolution in selection of the appropriate strain technique for evaluation of subclinical myocardial dysfunction. Echocardiography. 2012;29(3):334-9.

148. Xu TY, Sun JP, Lee AP, Yang XS, Qiao Z, Luo X, et al. Three-dimensional speckle strain echocardiography is more accurate and efficient than 2D strain in the evaluation of left ventricular function. International journal of cardiology. 2014;176(2):360-6.

149. Maffessanti F, Nesser HJ, Weinert L, Steringer-Mascherbauer R, Niel J, Gorissen W, et al. Quantitative evaluation of regional left ventricular function using three-dimensional

speckle tracking echocardiography in patients with and without heart disease. The American journal of cardiology. 2009;104(12):1755-62.

150. Marwick TH, Leano RL, Brown J, Sun JP, Hoffmann R, Lysyansky P, et al. Myocardial strain measurement with 2-dimensional speckle-tracking echocardiography: definition of normal range. JACC Cardiovascular imaging. 2009;2(1):80-4.

151. Yingchoncharoen T, Agarwal S, Popovic ZB, Marwick TH. Normal ranges of left ventricular strain: a meta-analysis. J Am Soc Echocardiogr. 2013;26(2):185-91.

152. Hare JL, Brown JK, Marwick TH. Association of myocardial strain with left ventricular geometry and progression of hypertensive heart disease. The American journal of cardiology. 2008;102(1):87-91.

153. Ng AC, Delgado V, Bertini M, van der Meer RW, Rijzewijk LJ, Shanks M, et al. Findings from left ventricular strain and strain rate imaging in asymptomatic patients with type 2 diabetes mellitus. Am J Cardiol. 2009;104(10):1398-401.

154. Holland DJ, Marwick TH, Haluska BA, Leano R, Hordern MD, Hare JL, et al. Subclinical LV dysfunction and 10-year outcomes in type 2 diabetes mellitus. Heart. 2015;101(13):1061-6.

155. Huang SH, Crowley LE, Jefferies HJ, Eldehni MT, Odudu A, McIntyre CW. The impact of hemodialysis on segmental and global longitudinal myocardial strain. Can J Cardiol. 2014;30(11):1422-8.

156. Yuda S, Fang ZY, Marwick TH. Association of severe coronary stenosis with subclinical left ventricular dysfunction in the absence of infarction. Journal of the American Society of Echocardiography : official publication of the American Society of Echocardiography. 2003;16(11):1163-70.

157. Edvardsen T, Rosen BD, Pan L, Jerosch-Herold M, Lai S, Hundley WG, et al. Regional diastolic dysfunction in individuals with left ventricular hypertrophy measured by

tagged magnetic resonance imaging--the Multi-Ethnic Study of Atherosclerosis (MESA). Am Heart J. 2006;151(1):109-14.

158. Montgomery DE, Puthumana JJ, Fox JM, Ogunyankin KO. Global longitudinal strain aids the detection of non-obstructive coronary artery disease in the resting echocardiogram. European heart journal cardiovascular Imaging. 2012;13(7):579-87.

159. Deng YB, Liu R, Wu YH, Xiong L, Liu YN. Evaluation of short-axis and long-axis myocardial function with two-dimensional strain echocardiography in patients with different degrees of coronary artery stenosis. Ultrasound Med Biol. 2010;36(2):227-33.

160. Reant P, Labrousse L, Lafitte S, Bordachar P, Pillois X, Tariosse L, et al. Experimental validation of circumferential, longitudinal, and radial 2-dimensional strain during dobutamine stress echocardiography in ischemic conditions. Journal of the American College of Cardiology. 2008;51(2):149-57.

161. Nucifora G, Schuijf JD, Delgado V, Bertini M, Scholte AJ, Ng AC, et al. Incremental value of subclinical left ventricular systolic dysfunction for the identification of patients with obstructive coronary artery disease. Am Heart J. 2010;159(1):148-57.

162. Choi JO, Cho SW, Song YB, Cho SJ, Song BG, Lee SC, et al. Longitudinal 2D strain at rest predicts the presence of left main and three vessel coronary artery disease in patients without regional wall motion abnormality. European journal of echocardiography : the journal of the Working Group on Echocardiography of the European Society of Cardiology. 2009;10(5):695-701.

163. Biering-Sorensen T, Hoffmann S, Mogelvang R, Zeeberg Iversen A, Galatius S, Fritz-Hansen T, et al. Myocardial strain analysis by 2-dimensional speckle tracking echocardiography improves diagnostics of coronary artery stenosis in stable angina pectoris. Circ Cardiovasc Imaging. 2014;7(1):58-65.

164. Smedsrud MK, Sarvari S, Haugaa KH, Gjesdal O, Orn S, Aaberge L, et al. Duration of myocardial early systolic lengthening predicts the presence of significant coronary artery disease. Journal of the American College of Cardiology. 2012;60(12):1086-93.

165. Shimoni S, Gendelman G, Ayzenberg O, Smirin N, Lysyansky P, Edri O, et al. Differential effects of coronary artery stenosis on myocardial function: the value of myocardial strain analysis for the detection of coronary artery disease. Journal of the American Society of Echocardiography : official publication of the American Society of Echocardiography. 2011;24(7):748-57.

166. Tsai WC, Liu YW, Huang YY, Lin CC, Lee CH, Tsai LM. Diagnostic value of segmental longitudinal strain by automated function imaging in coronary artery disease without left ventricular dysfunction. Journal of the American Society of Echocardiography : official publication of the American Society of Echocardiography. 2010;23(11):1183-9.

167. Ng AC, Sitges M, Pham PN, Tran da T, Delgado V, Bertini M, et al. Incremental value of 2-dimensional speckle tracking strain imaging to wall motion analysis for detection of coronary artery disease in patients undergoing dobutamine stress echocardiography. Am Heart J. 2009;158(5):836-44.

168. Dahlslett T, Karlsen S, Grenne B, Eek C, Sjoli B, Skulstad H, et al. Early assessment of strain echocardiography can accurately exclude significant coronary artery stenosis in suspected non-ST-segment elevation acute coronary syndrome. Journal of the American Society of Echocardiography : official publication of the American Society of Echocardiography. 2014;27(5):512-9.

169. Cusma-Piccione M, Zito C, Oreto L, D'Angelo M, Tripepi S, Di Bella G, et al. Longitudinal Strain by Automated Function Imaging Detects Single-Vessel Coronary Artery Disease in Patients Undergoing Dipyridamole Stress Echocardiography. Journal of the

American Society of Echocardiography : official publication of the American Society of Echocardiography. 2015;28(10):1214-21.

170. Shiran A, Blondheim DS, Shimoni S, Jabarren M, Rosenmann D, Sagie A, et al. Two-dimensional strain echocardiography for diagnosing chest pain in the emergency room: a multicentre prospective study by the Israeli echo research group. European heart journal cardiovascular Imaging. 2016.

171. Norum IB, Ruddox V, Edvardsen T, Otterstad JE. Diagnostic accuracy of left ventricular longitudinal function by speckle tracking echocardiography to predict significant coronary artery stenosis. A systematic review. BMC Med Imaging. 2015;15:25.

172. Lee M, Chang SA, Cho EJ, Park SJ, Choi JO, Lee SC, et al. Role of strain values using automated function imaging on transthoracic echocardiography for the assessment of acute chest pain in emergency department. The international journal of cardiovascular imaging. 2015;31(3):547-56.

173. Kleijn SA, Aly MF, Terwee CB, van Rossum AC, Kamp O. Three-dimensional speckle tracking echocardiography for automatic assessment of global and regional left ventricular function based on area strain. Journal of the American Society of Echocardiography : official publication of the American Society of Echocardiography. 2011;24(3):314-21.

174. Li L, Zhang PY, Ran H, Dong J, Fang LL, Ding QS. Evaluation of left ventricular myocardial mechanics by three-dimensional speckle tracking echocardiography in the patients with different graded coronary artery stenosis. The international journal of cardiovascular imaging. 2017.

175. Sun YJ, Wang F, Zhang RS, Wang HY, Yang CG, Cai J, et al. Incremental value of resting three-dimensional speckle-tracking echocardiography in detecting coronary artery disease. Exp Ther Med. 2015;9(6):2043-6.

176. Ternacle J, Gallet R, Champagne S, Teiger E, Gellen B, Dubois Rande JL, et al. Changes in three-dimensional speckle-tracking-derived myocardial strain during percutaneous coronary intervention. Journal of the American Society of Echocardiography : official publication of the American Society of Echocardiography. 2013;26(12):1444-9.

177. Einstein AJ, Moser KW, Thompson RC, Cerqueira MD, Henzlova MJ. Radiation dose to patients from cardiac diagnostic imaging. Circulation. 2007;116(11):1290-305.

178. Yun CH, Lin TY, Wu YJ, Liu CC, Kuo JY, Yeh HI, et al. Pericardial and thoracic peri-aortic adipose tissues contribute to systemic inflammation and calcified coronary atherosclerosis independent of body fat composition, anthropometric measures and traditional cardiovascular risks. European journal of radiology. 2012;81(4):749-56.

179. Nishimura RA, Miller FA, Jr., Callahan MJ, Benassi RC, Seward JB, Tajik AJ. Doppler echocardiography: theory, instrumentation, technique, and application. Mayo Clin Proc. 1985;60(5):321-43.

180. Tajik AJ, Seward JB, Hagler DJ, Mair DD, Lie JT. Two-dimensional real-time ultrasonic imaging of the heart and great vessels. Technique, image orientation, structure identification, and validation. Mayo Clin Proc. 1978;53(5):271-303.

181. Mosteller RD. Simplified calculation of body-surface area. N Engl J Med. 1987;317(17):1098.

182. Ng AC, Delgado V, Bertini M, van der Meer RW, Rijzewijk LJ, Hooi Ewe S, et al. Myocardial steatosis and biventricular strain and strain rate imaging in patients with type 2 diabetes mellitus. Circulation. 2010;122(24):2538-44.

183. Muraru D, Cucchini U, Mihaila S, Miglioranza MH, Aruta P, Cavalli G, et al. Left ventricular myocardial strain by three-dimensional speckle-tracking echocardiography in healthy subjects: reference values and analysis of their physiologic and technical

determinants. Journal of the American Society of Echocardiography : official publication of the American Society of Echocardiography. 2014;27(8):858-71 e1.

184. Greulich S, de Wiza DH, Preilowski S, Ding Z, Mueller H, Langin D, et al. Secretory products of guinea pig epicardial fat induce insulin resistance and impair primary adult rat cardiomyocyte function. J Cell Mol Med. 2011;15(11):2399-410.

185. Tumuklu MM, Etikan I, Kisacik B, Kayikcioglu M. Effect of obesity on left ventricular structure and myocardial systolic function: assessment by tissue Doppler imaging and strain/strain rate imaging. Echocardiography. 2007;24(8):802-9.

186. Ammar KA, Redfield MM, Mahoney DW, Johnson M, Jacobsen SJ, Rodeheffer RJ. Central obesity: association with left ventricular dysfunction and mortality in the community. Am Heart J. 2008;156(5):975-81.

187. Horwich TB, Fonarow GC. Glucose, obesity, metabolic syndrome, and diabetes relevance to incidence of heart failure. Journal of the American College of Cardiology. 2010;55(4):283-93.

188. Schrauwen-Hinderling VB, Hesselink MK, Meex R, van der Made S, Schar M, Lamb H, et al. Improved ejection fraction after exercise training in obesity is accompanied by reduced cardiac lipid content. The Journal of clinical endocrinology and metabolism. 2010;95(4):1932-8.

189. Levey AS, Coresh J, Greene T, Stevens LA, Zhang YL, Hendriksen S, et al. Using standardized serum creatinine values in the modification of diet in renal disease study equation for estimating glomerular filtration rate. Annals of internal medicine. 2006;145(4):247-54.

190. Voigt JU, Pedrizzetti G, Lysyansky P, Marwick TH, Houle H, Baumann R, et al. Definitions for a common standard for 2D speckle tracking echocardiography: consensus document of the EACVI/ASE/Industry Task Force to standardize deformation imaging.

Journal of the American Society of Echocardiography : official publication of the American Society of Echocardiography. 2015;28(2):183-93.

191. Ng AC, Goo SY, Roche N, van der Geest RJ, Wang WY. Epicardial Adipose Tissue Volume and Left Ventricular Myocardial Function Using 3-Dimensional Speckle Tracking Echocardiography. Can J Cardiol. 2016;32(12):1485-92.

192. Zuo H, Yan J, Zeng H, Li W, Li P, Liu Z, et al. Diagnostic power of longitudinal strain at rest for the detection of obstructive coronary artery disease in patients with type 2 diabetes mellitus. Ultrasound Med Biol. 2015;41(1):89-98.

APPENDIX

Metro South Health

Enquiries to: Centres For Health Research
Research Governance
Phone: (07) 3176 7722
Fax: (07) 3176 7667
Our Ref: HREC/12/QPAH/563 - SSA/12/QPAH/575
E-mail PAH-Research@health.qld.gov.au

Dr Arnold Ng
Princess Alexandra Hospital
Department of Cardiology
199 Ipswich Road
Woolloongabba Qld 4102

HREC APPROVAL AND SSA AUTHORISATION - PRINCESS ALEXANDRA HOSPITAL METRO SOUTH HOSPITAL AND HEALTH SERVICE

Dear Dr Ng,

HREC Reference number: HREC/12/QPAH/563
SSA reference number: SSA/12/QPAH/575
Project title: Left ventricular systolic function in patients who underwent cardiac computed tomography

I am pleased to advise that the above protocol has been recommended for approval by the Low and Negligible Risk Sub Committee of the Metro South Human Research Ethics Committee. The Committee is duly constituted, operates in accordance and complies with the current National Health and Medical Research Council's *National Statement on Ethical Conduct in Human Research 2007*.

On the recommendation of the Human Research Ethics Committee approval is granted for your project to proceed.

The duration of approval is 3 years from the date of this letter.

This approval is subject to researcher(s) compliance throughout the duration of the research with certain requirements as outlined in the *National Statement on Ethical Conduct in Human Research 2007 and Australian Code for the Responsible Conduct of Research.*

The following links have been provided for your convenience:
http://www.nhmrc.gov.au/publications/synopses/e72syn.htm
http://www.nhmrc.gov.au/publications/synopses/r39syn.htm

Some requirements are briefly outlined below. Please ensure that you communicate with the HREC on the following:

- ***Protocol Changes:*** Substantial changes made to the protocol require HREC approval http://www.health.qld.gov.au/pahospital/research/amendments.asp

- ***Problems and SAEs:*** The HREC must be informed of any problems that arise during the course of the study which may have ethical implications. Serious adverse events must be notified to the HREC as soon as possible http://www.health.qld.gov.au/pahospital/research/adverse_events.asp
- ***Lapsed Approval***: If the study has not commenced within twelve months approval will lapse requiring resubmission of the study to the HREC.
- ***Annual Reviews:*** All studies are required by the NHMRC to be reviewed annually. To assist with reporting obligations an Annual Report template is available on the MSHSD HREC website. This form is required to be completed and returned to the HREC within the 12 month reviewing period http://www.health.qld.gov.au/pahospital/research/monitoring.asp

If this research involves the recruitment of patients from the Metro South Hospital and Health Service (MSHHS), it is my responsibility to remind you of your ongoing duty of care for all people recruited into projects or clinical trials whilst public patients. All conditions and requirements regarding confidentiality of public information and patient privacy apply. You are required to comply at all times with any application requirements of Australian and Queensland Laws including the Health Services Act, the Privacy Act, Public Health Act (2005) and other relevant legislation, ethics obligations and guidelines which may be applicable to the MSHHS from time to time including, without limitation, any requirement in respect of the maintenance, preservation or destruction of patient records.

When the study involves patient contact, it is your responsibility as the principal investigator to notify the relevant consultant and request their approval.

Should you have any problems, please liaise directly with the Chair of the HREC early in the program.

A copy of this letter should be presented when required as official confirmation of the approval of the Metro South Human Research Ethics Committee.

We wish you every success in undertaking this research.

Yours sincerely,

Dr Richard Ashby
HEALTH SERVICE CHIEF EXECUTIVE
METRO SOUTH HEALTH
25 / 11 / 12

Office
Centres for Health Research
Princess Alexandra Hospital
Metro South Hospital and Health Service

Postal
Ipswich Road
Woolloongabba Q 4102

Phone
61 7 3176 7672

Fax
61 7 3176 7667